Electronic Supplementary Material (ESI) for Organic & Biomolecular Chemistry

Supporting Information

Highly Efficient Aldol additions of DHA and DHAP to *N*-Cbz-Aminoaldehydes Catalyzed by L-Rhamnulose-1-Phosphate and L-Fuculose-1-Phosphate Aldolases in Aqueous Borate Buffer

Xavier Garrabou[a], Jesús Joglar[a], Teodor Parella[b], Jordi Bujons[a] and Pere Clapés[a*]

[a]Dept Biological Chemistry and Molecular Modeling. Instituto de Química Avanzada de Cataluña, IQAC-CSIC. Jordi Girona 18-26, 08034 Barcelona, Spain.

[b]Servei de Ressonància Magnètica Nuclear, Departament de Química. Universitat Autònoma de Barcelona, Bellaterra, Spain.

Corresponding author

Prof. Dr. Pere Clapés
Catalonia Institute for Advanced Chemistry-CSIC
Jordi Girona 18-26,
08034 Barcelona,
Spain
Fax: +34932045904
Phone: +34934006112
email. pere.clapes@iqac.csic.es

Table S1. L-Rhamnulose-1-phosphate aldolase catalyzed aldol addition reactions of DHA-borate, DHAP and DHAP/borate buffer to *N*-Cbz-amino aldehydes (**1**).

Entry	Aldehyde	%[a]		Entry	Aldehyde	%[a]	
		DHA-Borate[b]	DHAP			DHA-Borate[b]	DHAP
1	**1a**	91	80[c]	10	(*S*)-**1f**	93	80[d]
2	(*S*)-**1b**	99	61[c]	11	(*R*)-**1f**	93	47[d]
3	(*R*)-**1b**	95	60[c]	12	(*S*)-**1g**	89	71[d]
4	(*S*)-**1c**	94	77[d]	13	(*S*)-**1h**	42	63[d]
5	(*R*)-**1c**	99	64[d]	14	(*R*)-**1h**	52	70[d]
6	(*S*)-**1d**	94	99[d]	15	**1i**	99	18[d]
7	(*R*)-**1d**	91	90[d]	16	**1j**	94	58[c]
8	(*S*)-**1e**	62	92[d]	17	(*S*)-**1k**	95	58[e]
9	(*R*)-**1e**	64	99[d]	18	(*R*)-**1k**	nr	69[e]

[a]Percentage of aldol adduct **2** formed respect to the limiting substrate, i.e. acceptor aldehyde. The amount of product was measured by HPLC peak integration using an external standard method.

[b]Reaction conditions: [Aldehyde] = 65 mM; [DHA] = 100 mM; RhuA = 0.6 U; volume of the mixture 300 µL; 200 mM borate buffer pH 7.5. Percentage of aldol adduct measured after 24 h.

[c]Reaction conditions: [DHAP] = 90 mM; [Aldehyde] = 144 mM, DHAP adjusted to pH 6.9, no buffer added, 25 ºC, RhuA = 2.5 U; volume of the reaction mixture 2.5 mL. Reaction time: 2-3 h. Data from Espelt et al.[1]

[d]Reaction conditions: [DHAP] = 50 mM; [Aldehyde] = 85 mM, DHAP adjusted to pH 6.9, no buffer added, 25 ºC, RhuA = 5 U; volume of the reaction mixture 2.5 mL.

Percentage of aldol adduct **2** measured at the time when no apparent change in reactant and product concentrations: 24-48 h. Data from Calveras et al.[2]

[e]Reaction conditions: [DHAP] = 78 mM; [Aldehyde] = 136 mM, DHAP adjusted to pH 6.9, no buffer added, 25 ºC, RhuA = 1.5 U; volume of the reaction mixture 2.8 mL. Percentage of aldol adduct **2** at 44 h. Data from Calveras et al.[3]; for the stereochemistry of these aldol additions see Garrabou et al.[4]

nr: no reaction.

Table S2. L-Rhamnulose-1-phosphate aldolase catalyzed aldol addition reactions of DHAP and DHAP with borate buffer to *N*-Cbz-amino aldehydes (**1**).

Entry	Aldehyde	%[a]		Entry	Aldehyde	%[a]	
		DHAP/Borate[b]	DHAP[b]			DHAP/Borate[b]	DHAP[b]
1	**1a**	59	80	6	(*S*)-**1g**	79	71
2	(*S*)-**1b**	91	61	7	(*S*)-**1h**	80	63
3	(*R*)-**1b**	82	60	8	(*R*)-**1h**	75	70
4	(*S*)-**1f**	74	80	9	(*S*)-**1k**	77	58
5	(*R*)-**1f**	42	47	10	(*R*)-**1k**	62	69

[a]Percentage of aldol adduct **2** formed respect to the limiting substrate, DHAP. The amount of aldol adduct formed was determined by HPLC using an external standard method.

[b]Reactions were conducted at 4 ºC in borate buffer 200 mM, pH 7.0 or adjusted to pH 6.9-7.0 without any other buffer solution added. [DHAP] = 40 mM; [aldehyde] = 68 mM, volume = 360 µL, RhuA wild-type = 0.72 U; conversions measured after 24 hours.

Preparation of a solution of FucA F131A. A solution (50 mL) containing FucA F131A freshly eluted from an affinity column was obtained as described.[4] A fraction of this solution (15 mL) was dialyzed twice against 5 L of buffer (50 mM triethanolamine·HCl pH 7.0, 10 mM NH_4SO_4, 50 mM NaCl, 10 μM $ZnCl_2$) for 12 h at 4 ºC. The concentration of protein in solution (4.0 mg protein mL^{-1}) was established using the Bradford methodology.[5] The resulting enzyme preparation was used directly in the reactions (0.812 mg of FucA F131A mL^{-1} of reaction, 0.18 U mg^{-1} protein, 0.15 U mL^{-1} of reaction) at analytical scale.

The FucA catalysts used were stored as ammonium sulphate suspensions, which was the most convenient way to stabilize them for long periods. To exclude any possible effect of the enzyme preparation on the activity with and without borate buffer, experiments were conducted using freshly purified FucA, prepared as indicated above, in which the precipitation step with ammonium sulphate was avoided (see experimental section). The results show a similar enhancement of the reaction kinetics when carried out in borate buffer relative to those carried out in TEA buffer, indicating that there was no effect due to the enzyme preparation (Table 2).

Table S3. Initial reaction rates (v_o μmol aldol adduct formed h^{-1} mg^{-1}) of the aldol addition reaction of DHAP to (*R*)-**1h** and (*S*)-**1h** catalyzed by L-fuculose-1-phosphate aldolase at 25 ºC.

Aldehyde acceptor	FucA catalyst	pH	v_o (μmol h^{-1} mg^{-1})[a]	
			Borate	Triethanolamine
(*R*)-**1h**	F131A[b]	7.0	119	37
(*S*)-**1h**	wild type[c]	7.0	17	2.5
(*S*)-**1h**	F131A[c]	7.0	50	12

[a]Reactions were conducted at 25 ºC using borate buffer 200 mM, TEA 50 mM adjusted to pH 7.0. [DHAP] = 50 mM; [(*R*)-**1h**] = [(*S*)-**1h**] = 65 mM, volume = 300 μL. Values are the mean of three determinations with a standard error between 11-13 %.

[b]Freshly prepared = 0.05 U

[c]FucA wild-type

[d]FucA F131A

Figure S1. [1]HNMR, COSY, HSQC and NOESY spectra of the aldol adduct (3*R*,4*S*,5*S*)-**1b** at 263 K. Spectra recorded in [D4]MeOH.

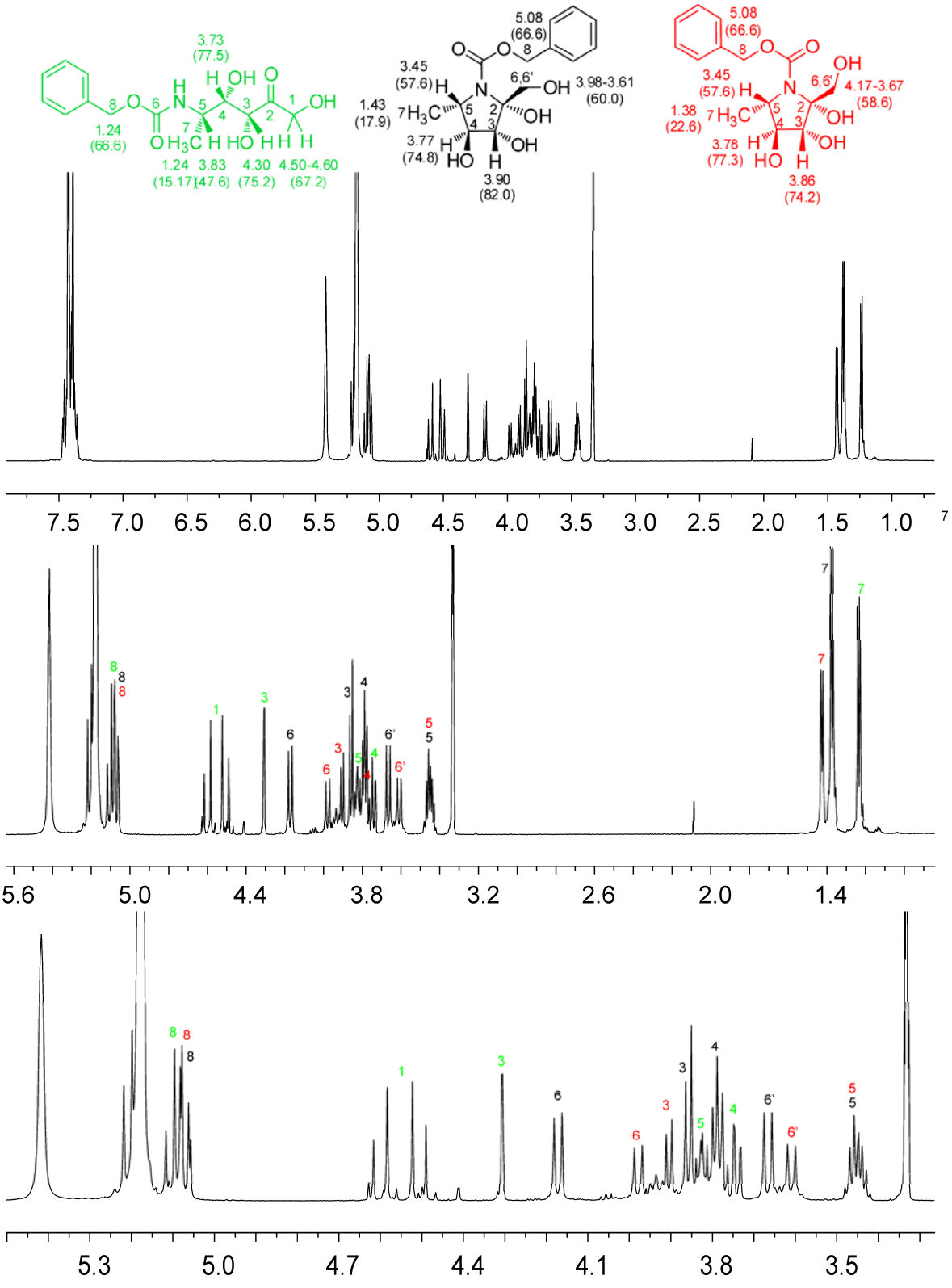

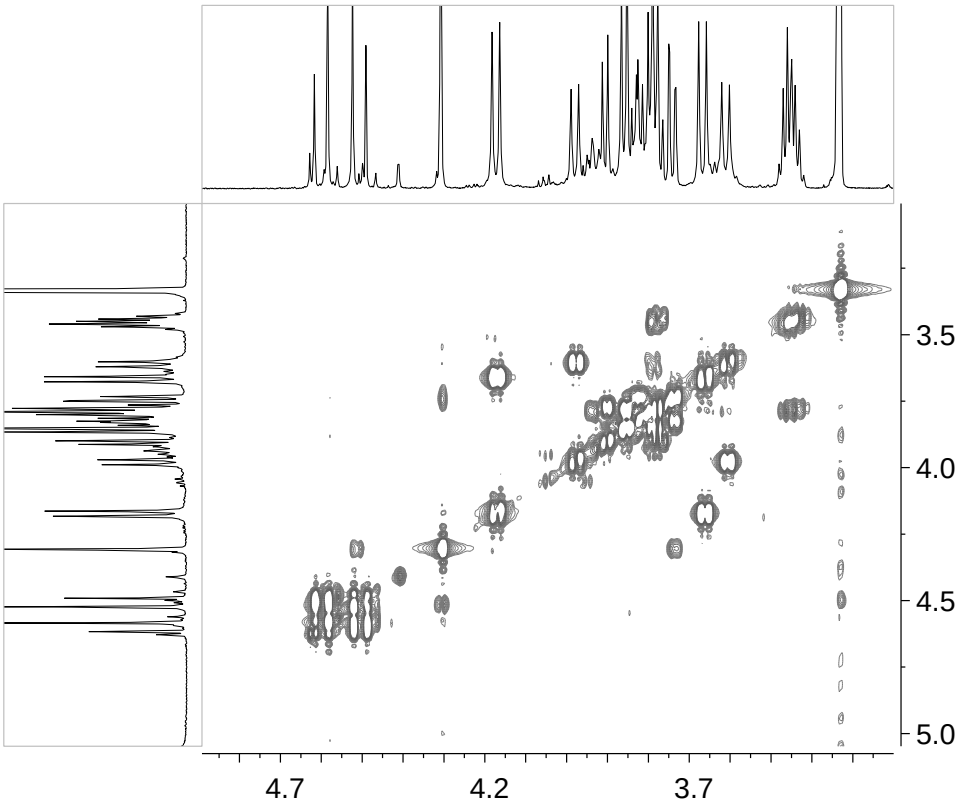

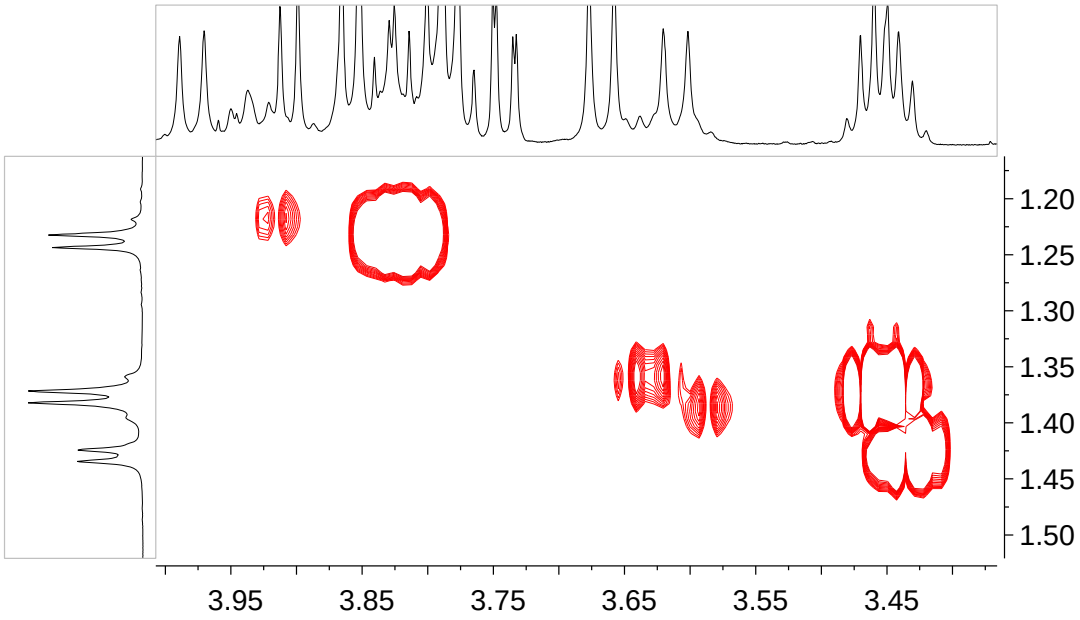

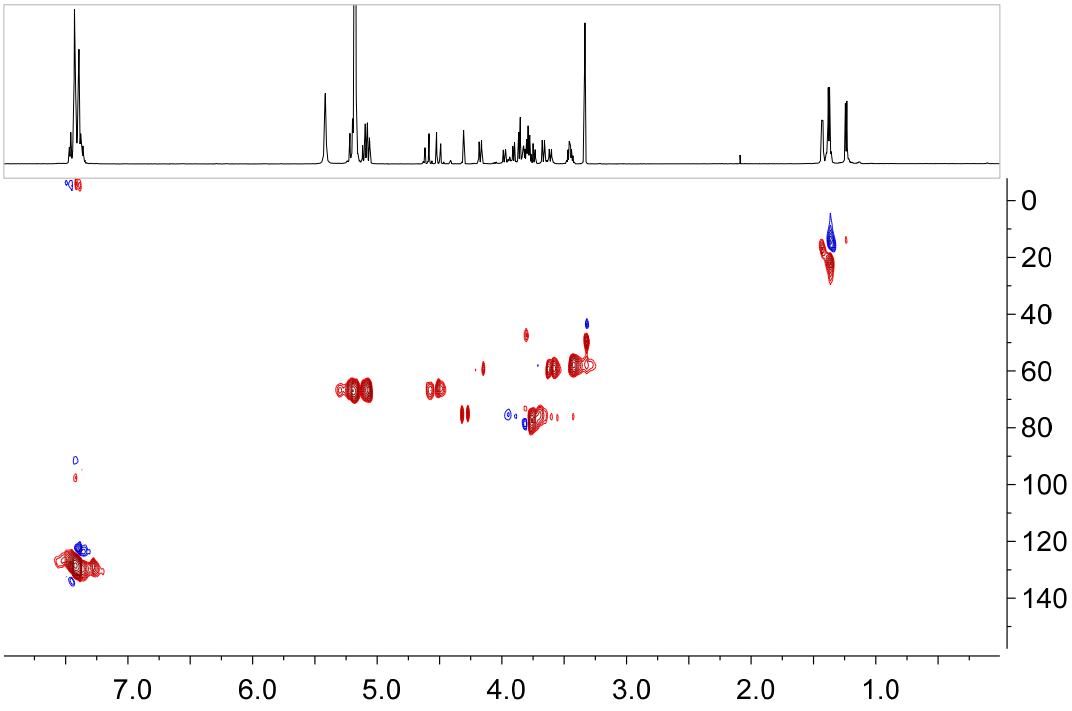

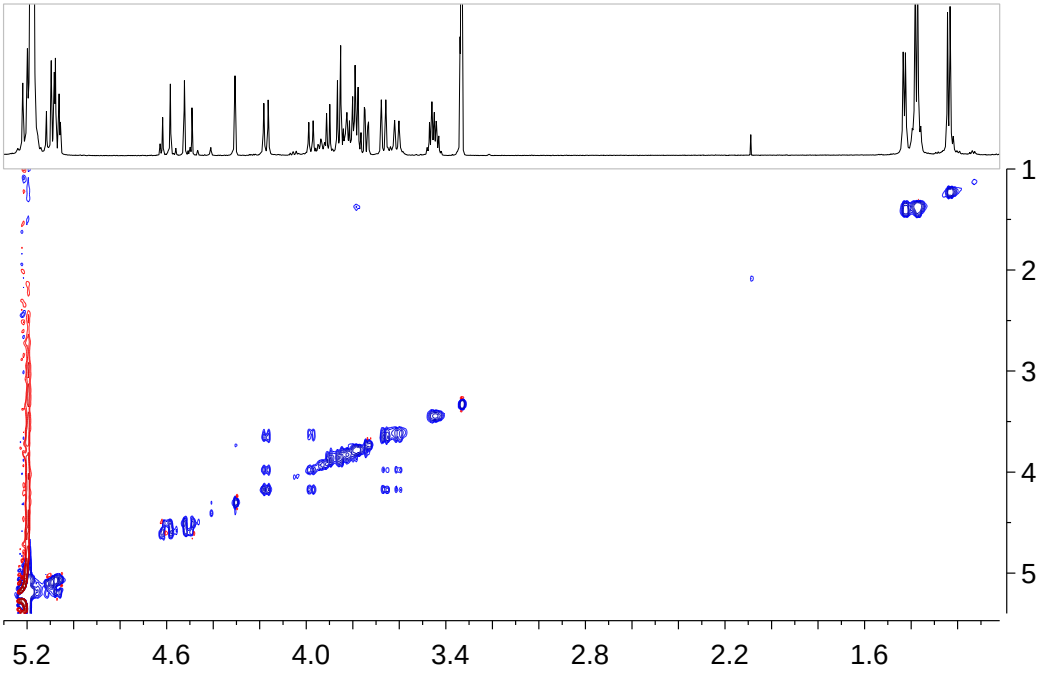

Figure S2. ^{1}HNMR spectra of the 1,4-dideoxy-1,4-imino-L-arabinitol (LAB) obtained from the aldol adduct that resulted from the aldol addition reaction of DHA to **1a** in the presence of borate.

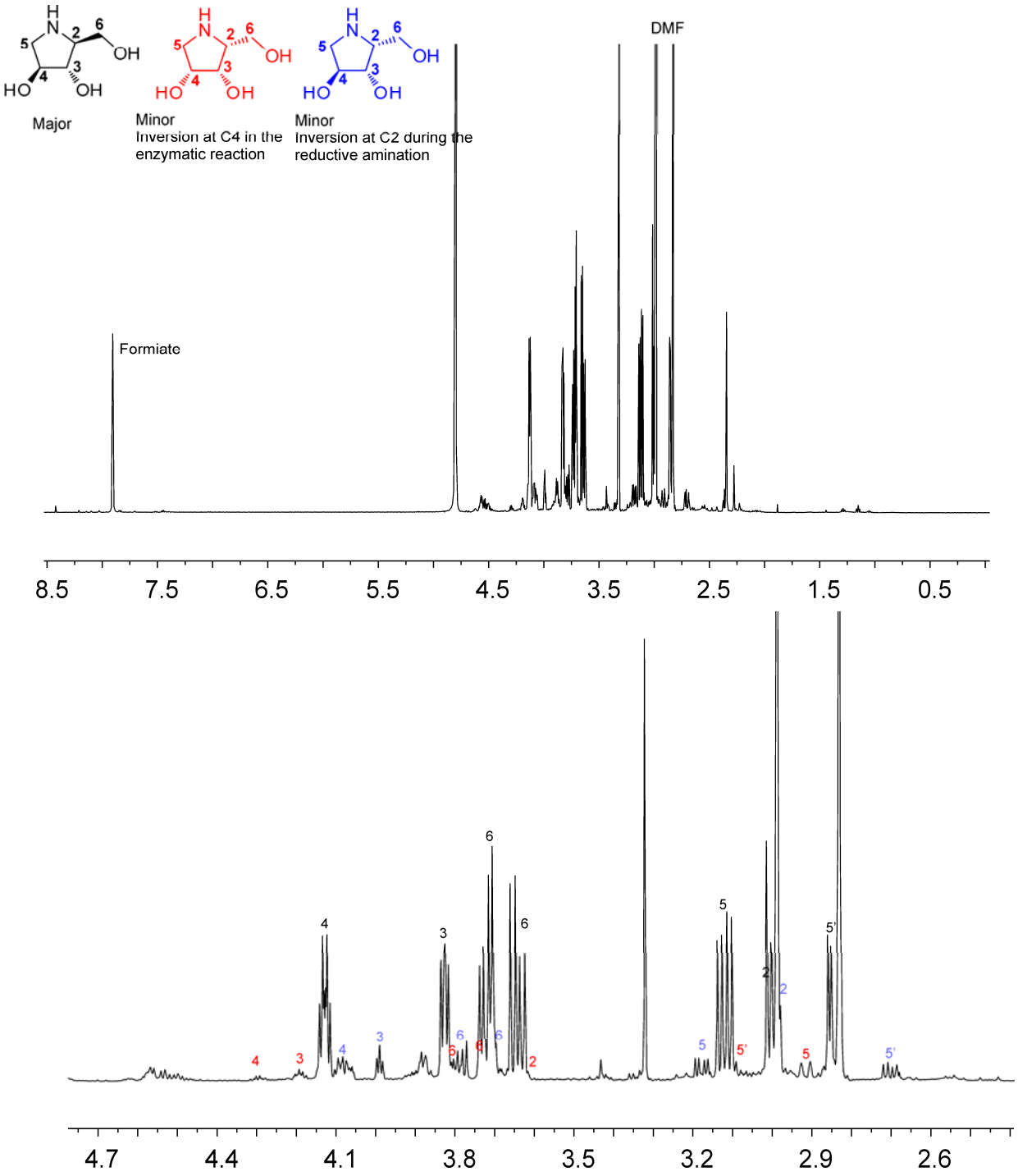

Figure S3. HPLC chromatograms of the aldol additions of DHAP and DHA in borate to (*R*)-**1b**. Phosphorylated adducts were treated with acid phosphatase before HPLC analysis following previously described procedures.[4] (a) aldol addition of DHAP to (*R*)-**1b** catalyzed by L-rhanmnulose-1-phosphate aldolase (RhuA); (b) aldol addition of DHA to (*R*)-**1b** catalyzed by RhuA in the presence of borate; (c) aldol addition of DHAP to (*R*)-**1b** catalyzed by L-fuculose-1-phosphate aldolase (FucA). Blank chromatogram: reaction without enzyme added.

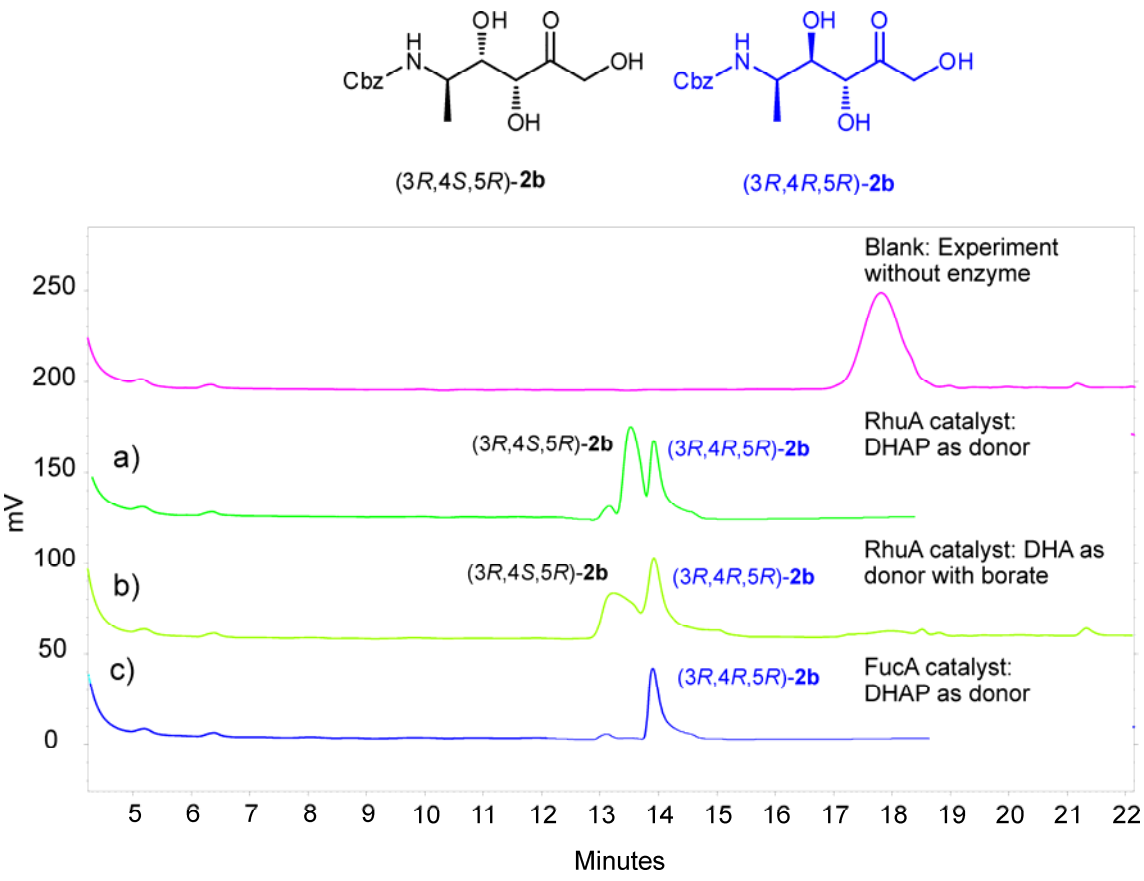

Figure S4. HPLC chromatograms of the aldol additions of DHAP and DHA in borate to (*S*)-**1f**. Phosphorylated adducts were treated with acid phosphatase before HPLC analysis following previously described procedures.[4] (a) aldol addition of DHAP to (*S*)-**1f** catalyzed by L-rhanmnulose-1-phosphate aldolase (RhuA); (b) aldol addition of DHA to (*S*)-**1f** catalyzed by RhuA in the presence of borate; (c) aldol addition of DHAP to (*S*)-**1f** catalyzed by L-fuculose-1-phosphate aldolase (FucA). Blank chromatogram: reaction without enzyme added.

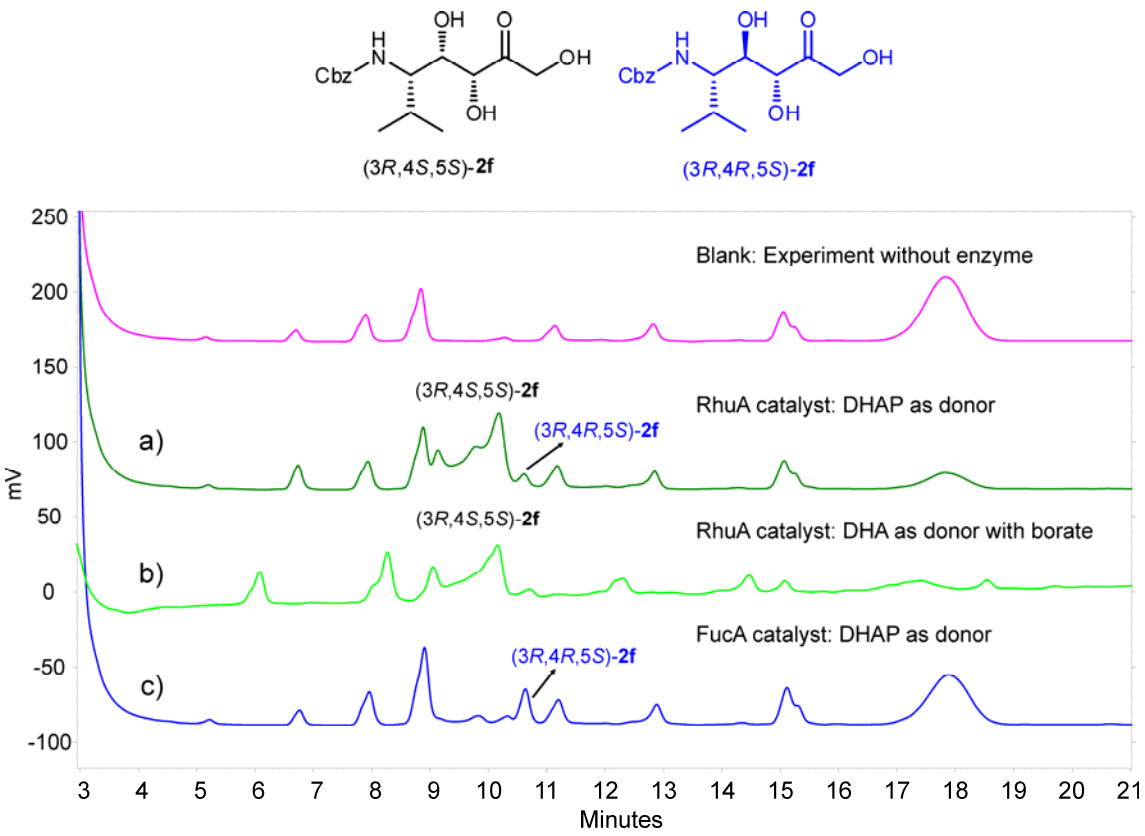

Figure S5. HPLC chromatograms of the aldol additions of DHAP and DHA in borate to (*S*)-**1g**. Phosphorylated adducts were treated with acid phosphatase before HPLC analysis following previously described procedures.[4] (a) aldol addition of DHAP to (*S*)-**1g** catalyzed by L-rhanmnulose-1-phosphate aldolase (RhuA); (b) aldol addition of DHA to (*S*)-**1g** catalyzed by RhuA in the presence of borate; (c) aldol addition of DHAP to (*S*)-**1g** catalyzed by L-fuculose-1-phosphate aldolase (FucA). Blank chromatogram: reaction without enzyme added.

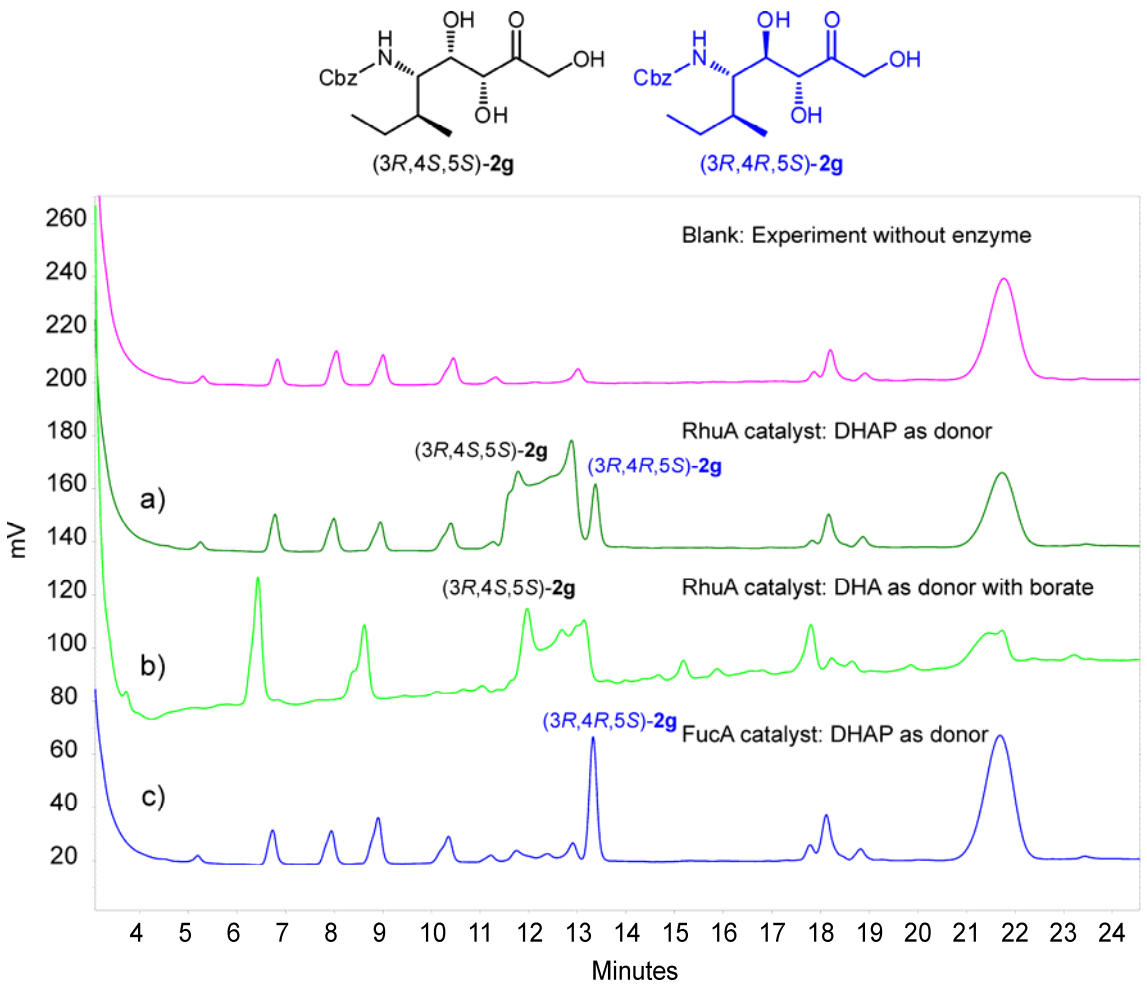

Figure S6. HPLC chromatograms of the aldol additions of DHAP and DHA with borate to (*S*)-**1h**. Phosphorylated adducts were treated with acid phosphatase before HPLC analysis following previously described procedures.[4] (a) aldol addition of DHAP to (*S*)-**1h** catalyzed by L-rhanmnulose-1-phosphate aldolase (RhuA); (b) aldol addition of DHA to (*S*)-**1h** catalyzed by RhuA in the presence of borate; (c) aldol addition of DHAP to (*S*)-**1h** catalyzed by L-fuculose-1-phosphate aldolase (FucA). Blank chromatogram: reaction without enzyme added.

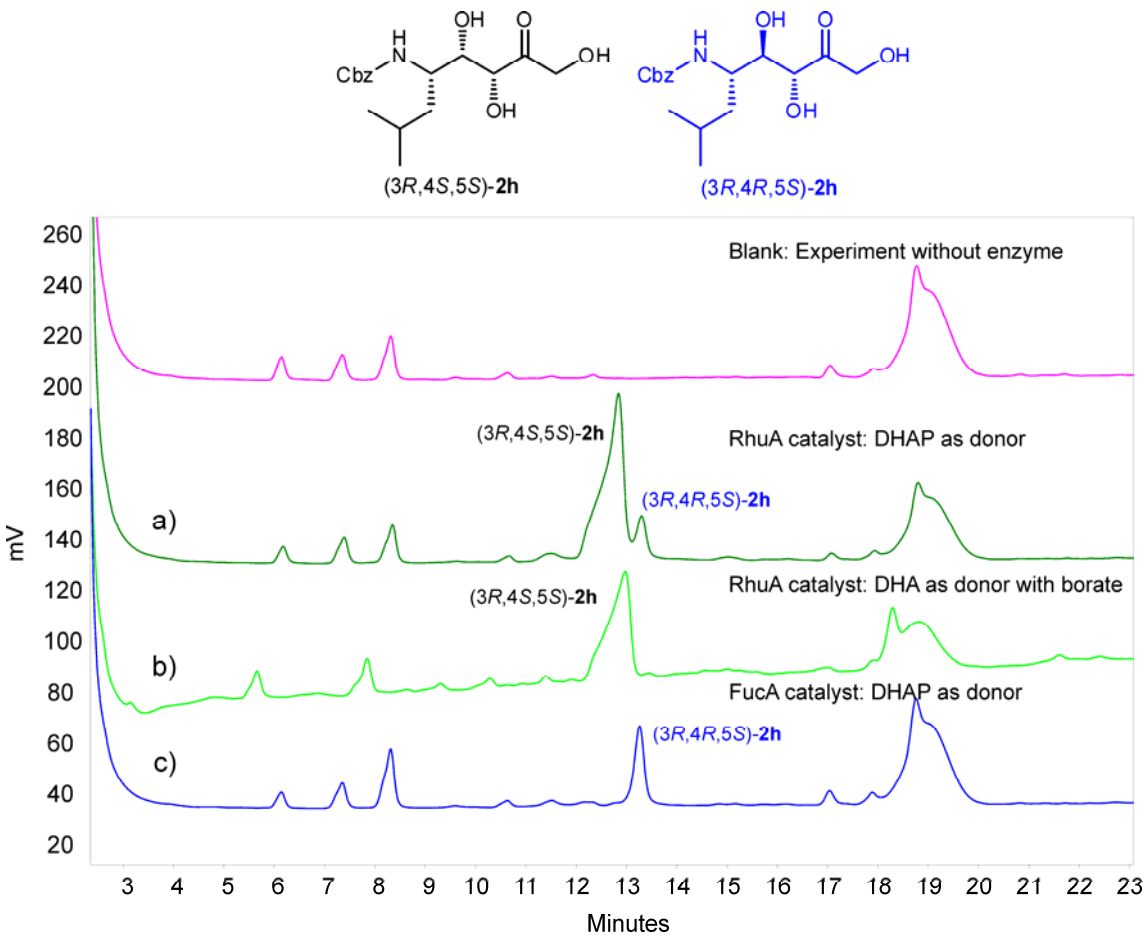

Figure S7. HPLC chromatograms of the aldol additions of DHAP and DHA with borate to (*S*)-**1k**. Phosphorylated adducts were treated with acid phosphatase before HPLC analysis following previously described procedures.[4] (a) aldol addition of DHAP to (*S*)-**1k** catalyzed by L-rhanmnulose-1-phosphate aldolase (RhuA); (b) aldol addition of DHA to (*S*)-**1k** catalyzed by RhuA in the presence of borate. Blank chromatogram: reaction without enzyme added.

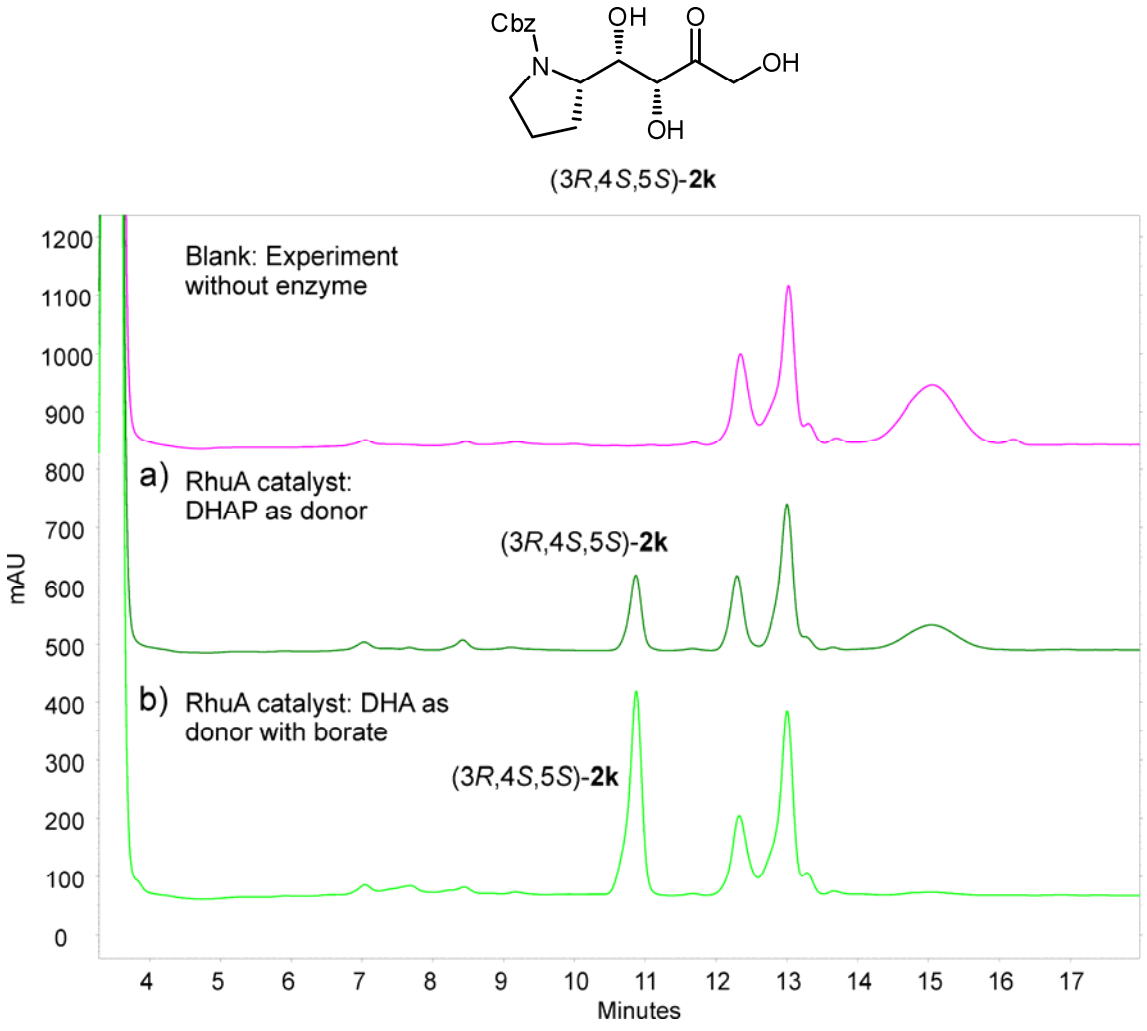

Figure S8. Observed ^{1}H and ^{13}C NMR spectra of the iminocyclitol resulted from the reductive amination of the aldol adduct from the aldol addition of DHA to (*S*)-**1c** catalyzed by RhuA in the presence of borate.

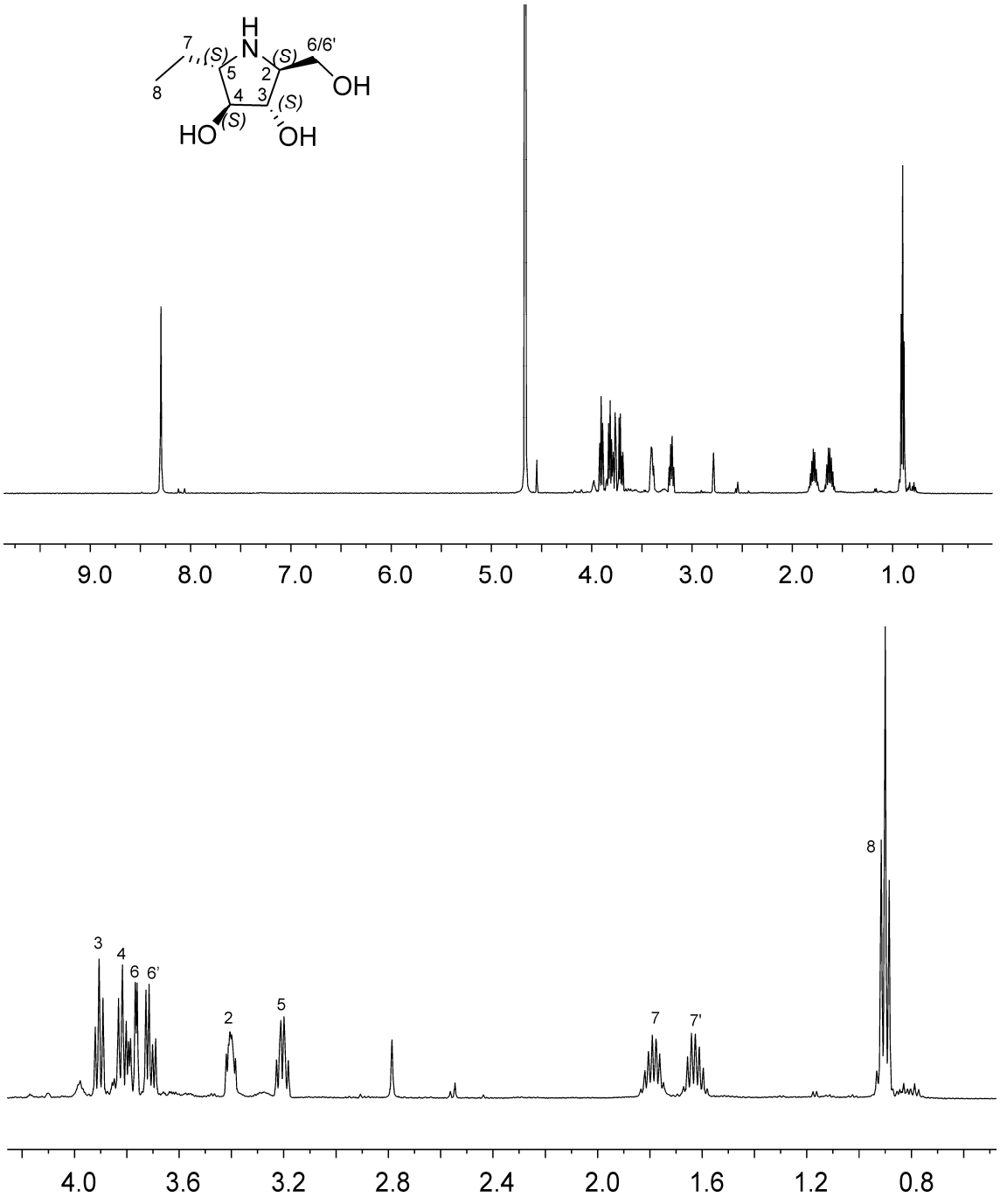

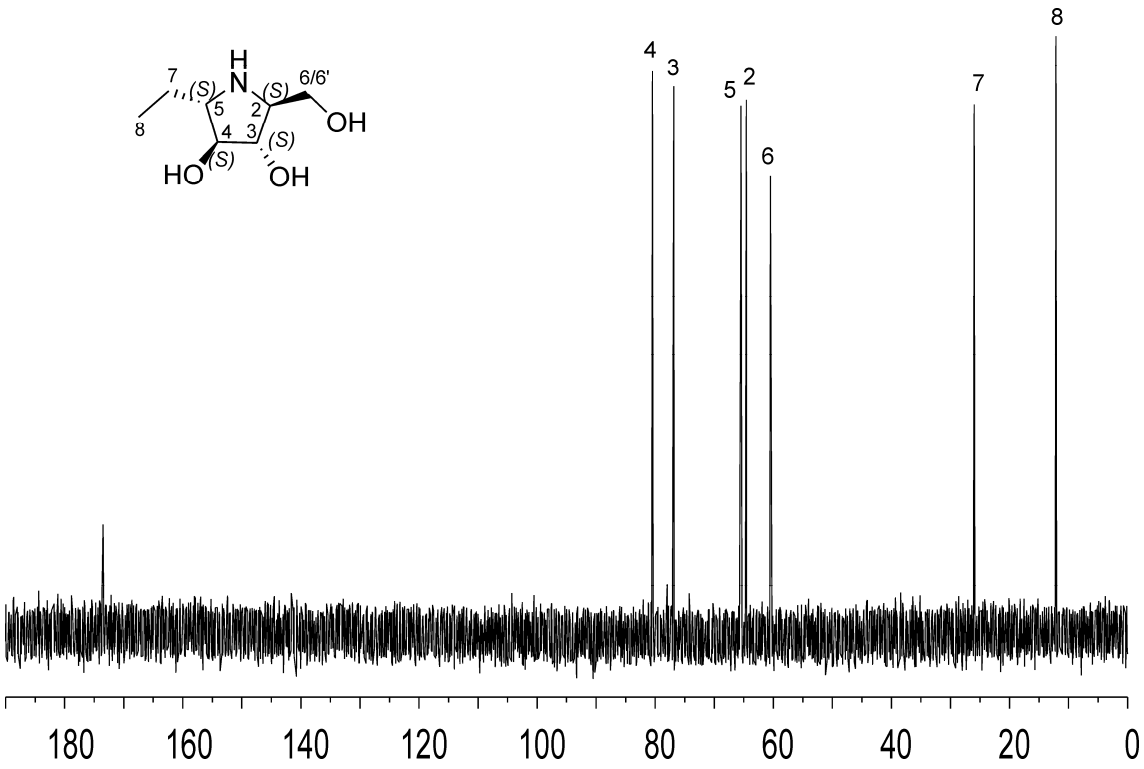
H
N
7
(S)
5
8
2
(S)
6/6'
OH
4
3
(S)
HO
(S)
OH
4
3
5
2
6
7
8
180
160
140
120
100
80
60
40
20
0

Figure S9. NMR spectra of the iminocyclitol resulted from the reductive amination of the aldol adduct from the aldol addition of DHA to (*R*)-**1c** catalyzed by RhuA in the presence of borate.

A) Observed ^{1}H and ^{13}C NMR.

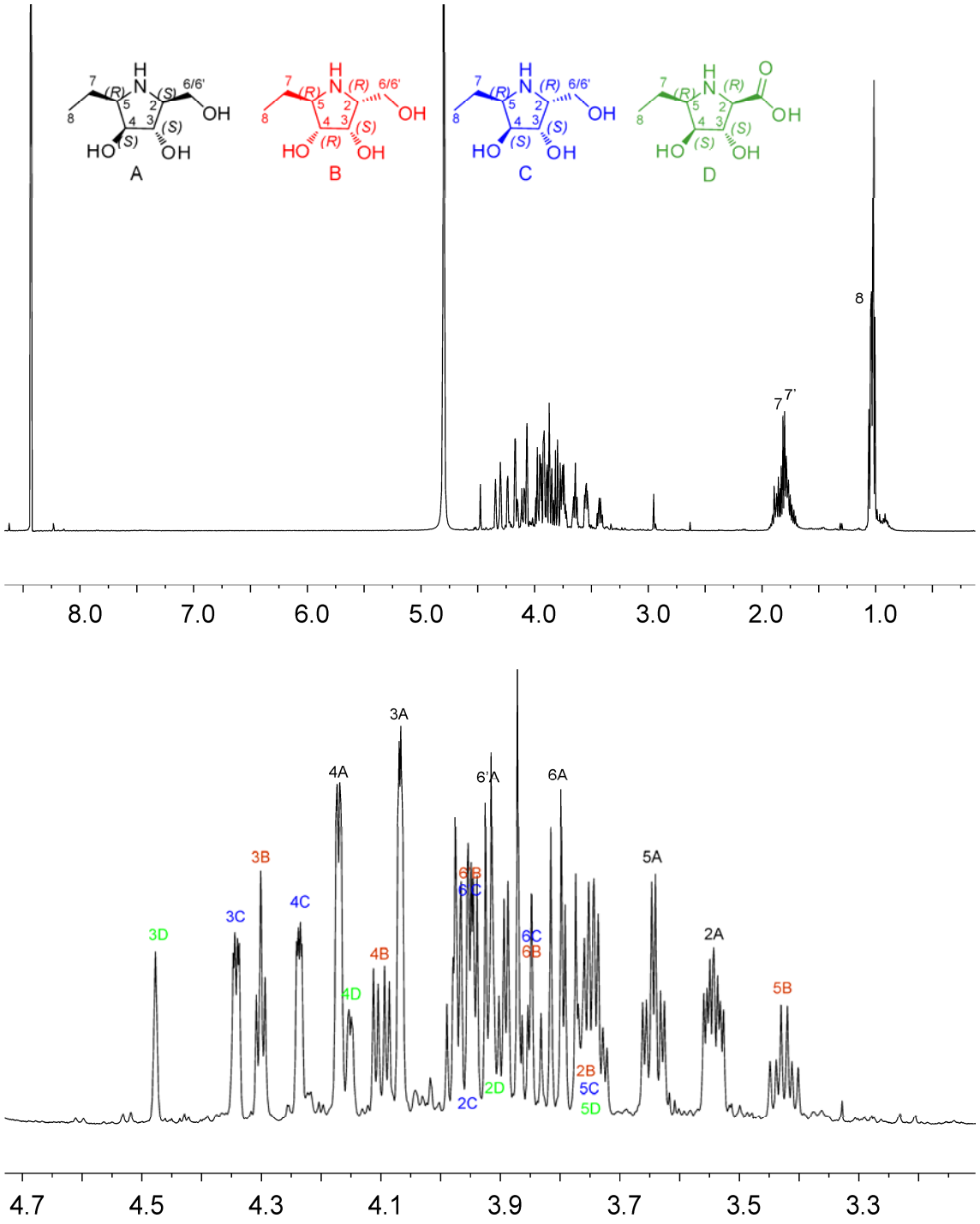

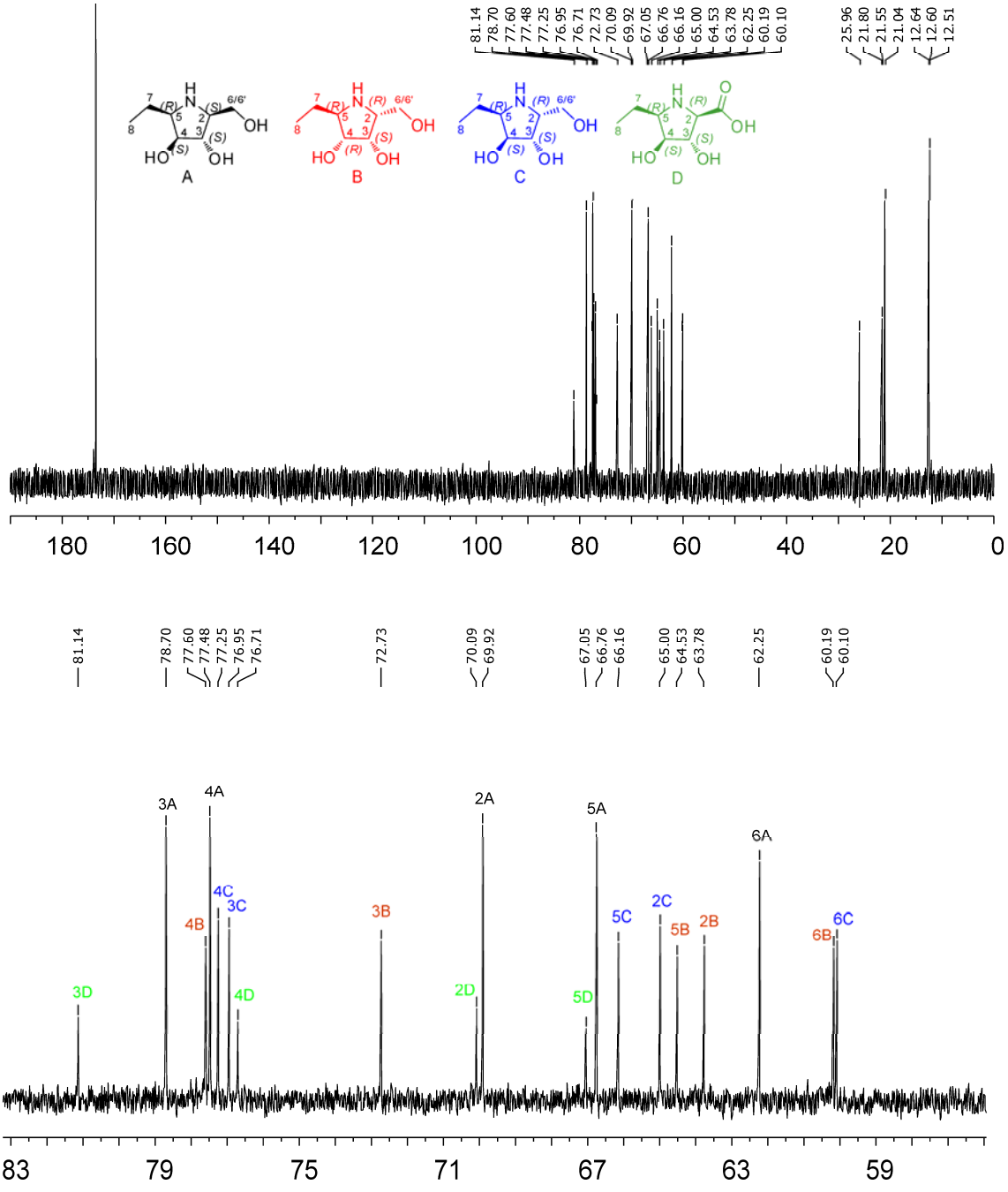

B) 2D ^{1}H-^{1}H COSY.

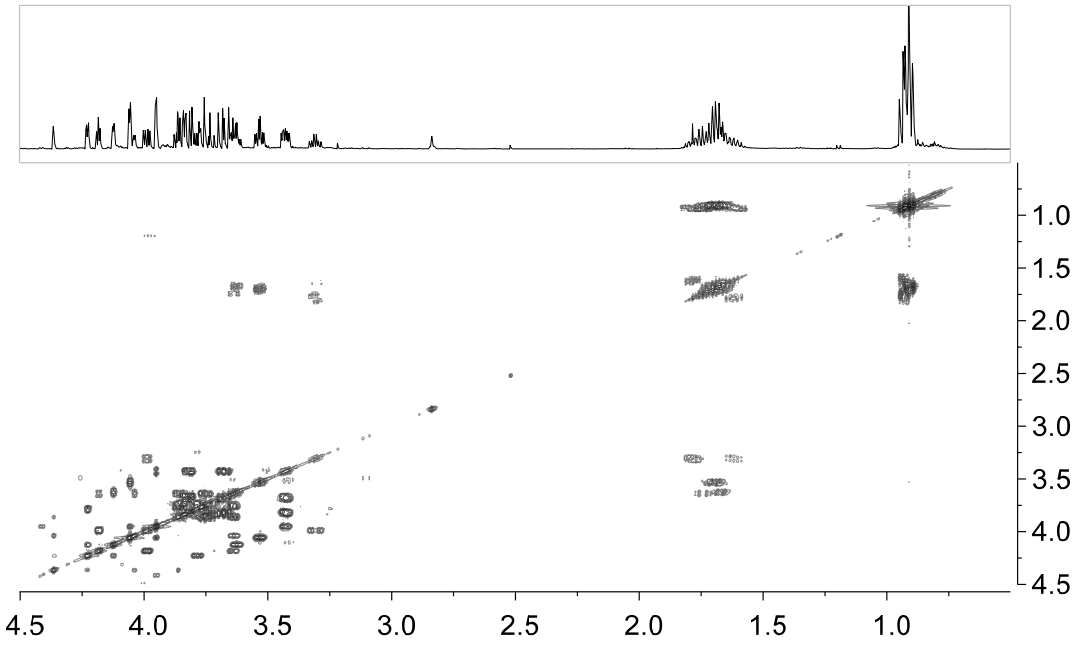

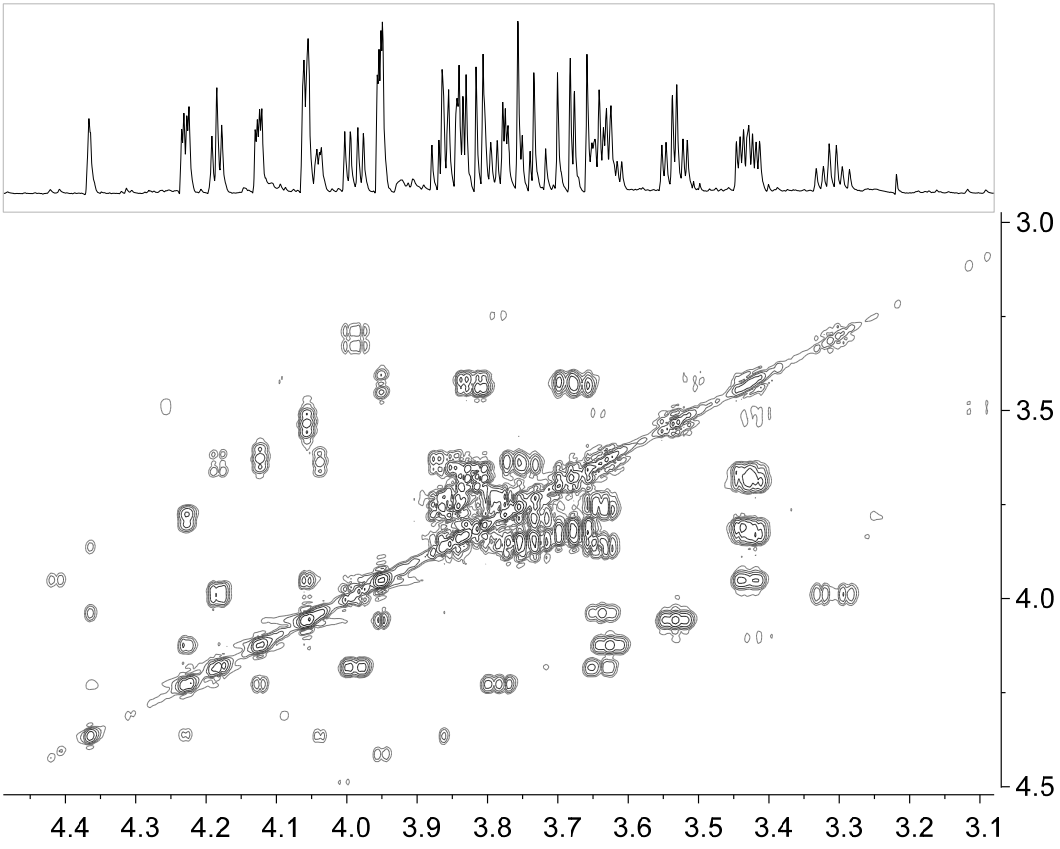

C) 2D multiplicity-edited HSQC.

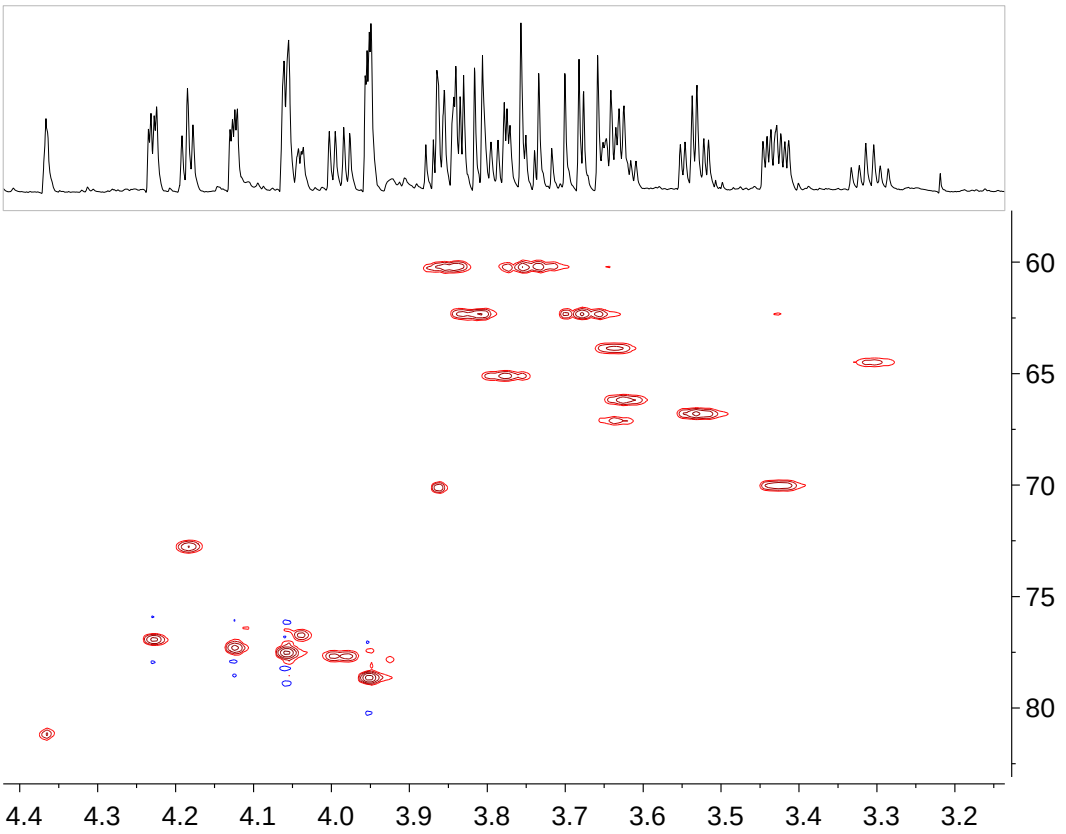

D) Magnitude mode ge-2D, ^{1}H-^{13}C HMBC

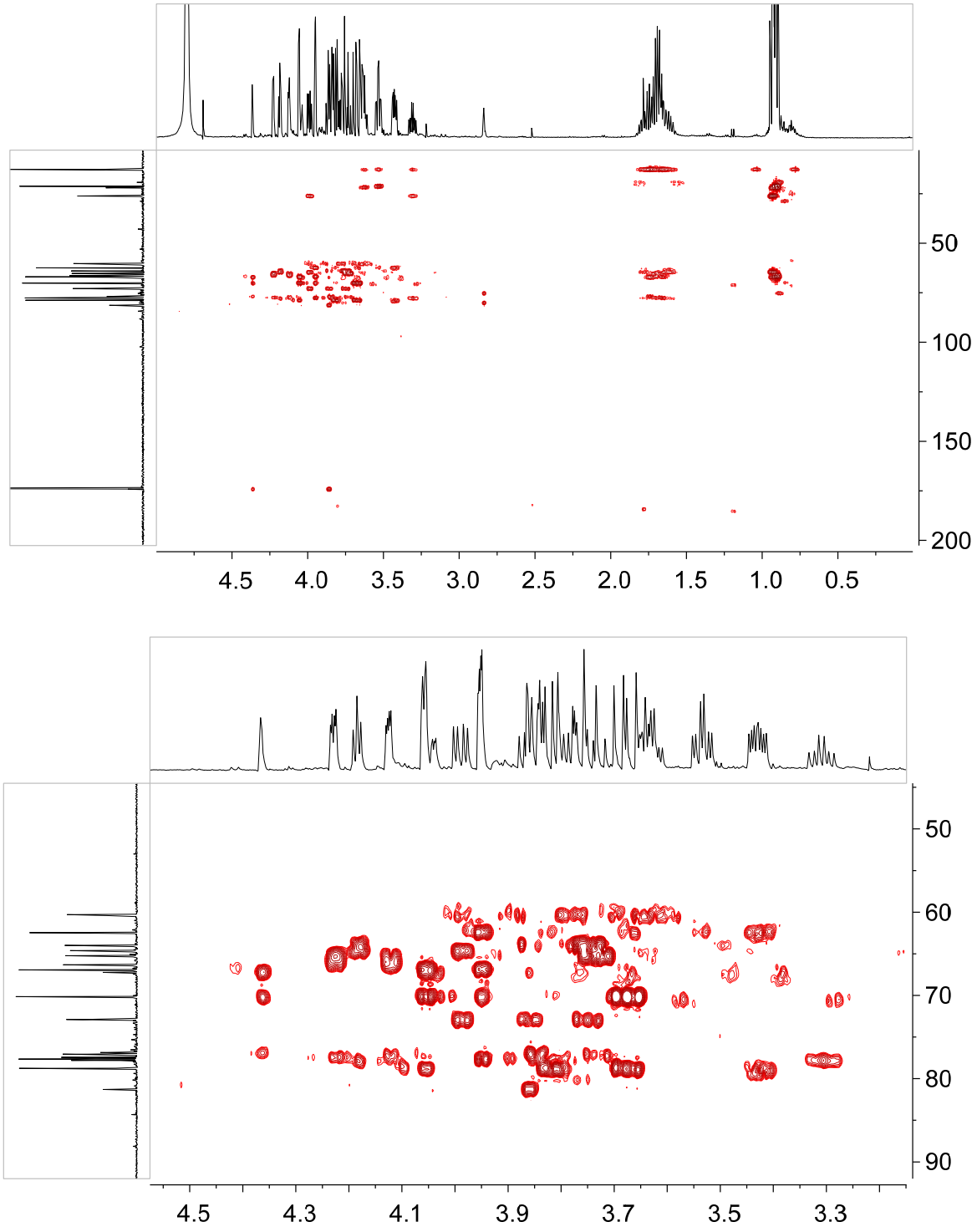

Figure S10. Observed ^{1}H and ^{13}C NMR spectra of the iminocyclitol resulted from the reductive amination of the aldol adduct from the aldol addition of DHA to (*S*)-**1d** catalyzed by RhuA in the presence of borate.

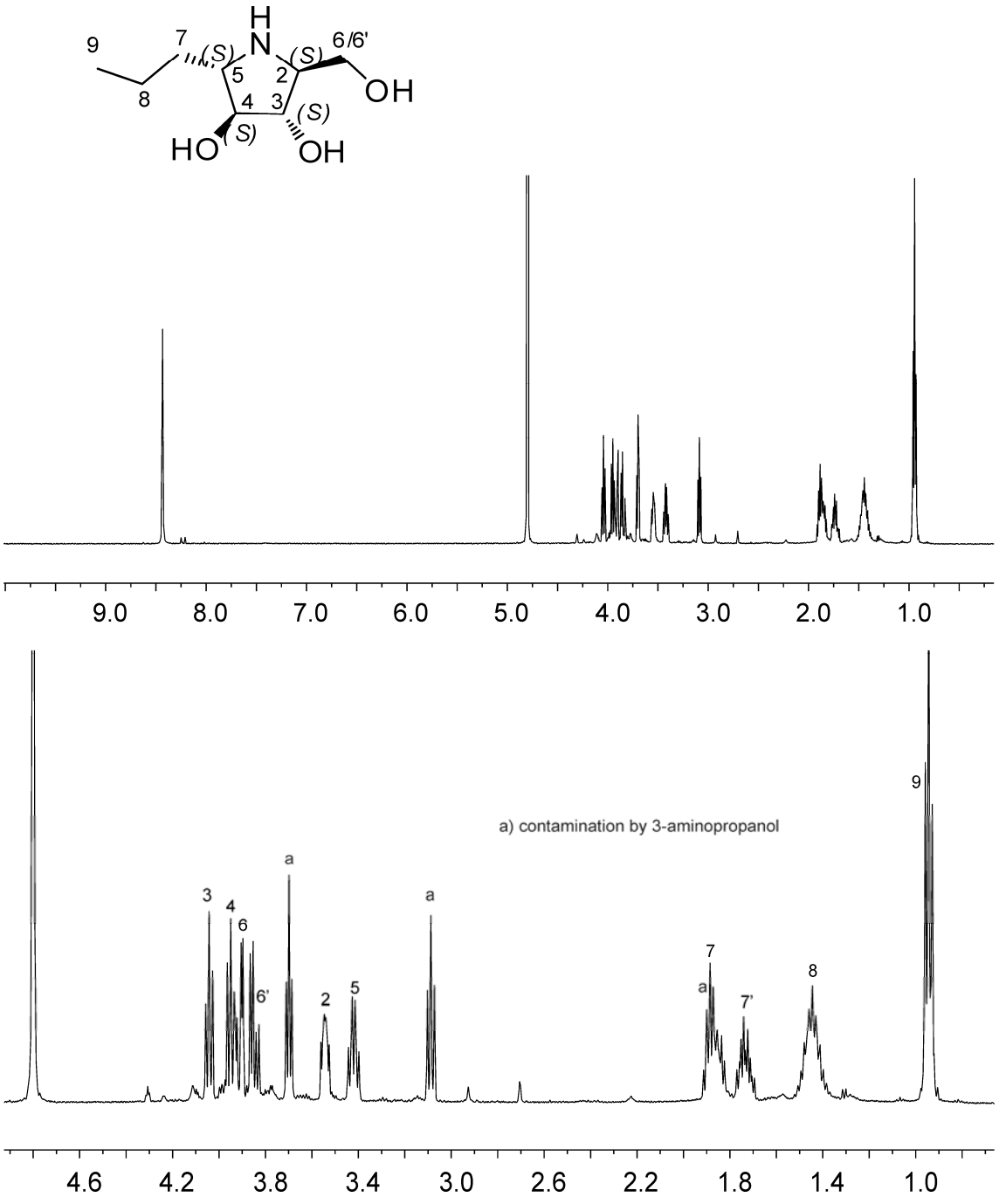

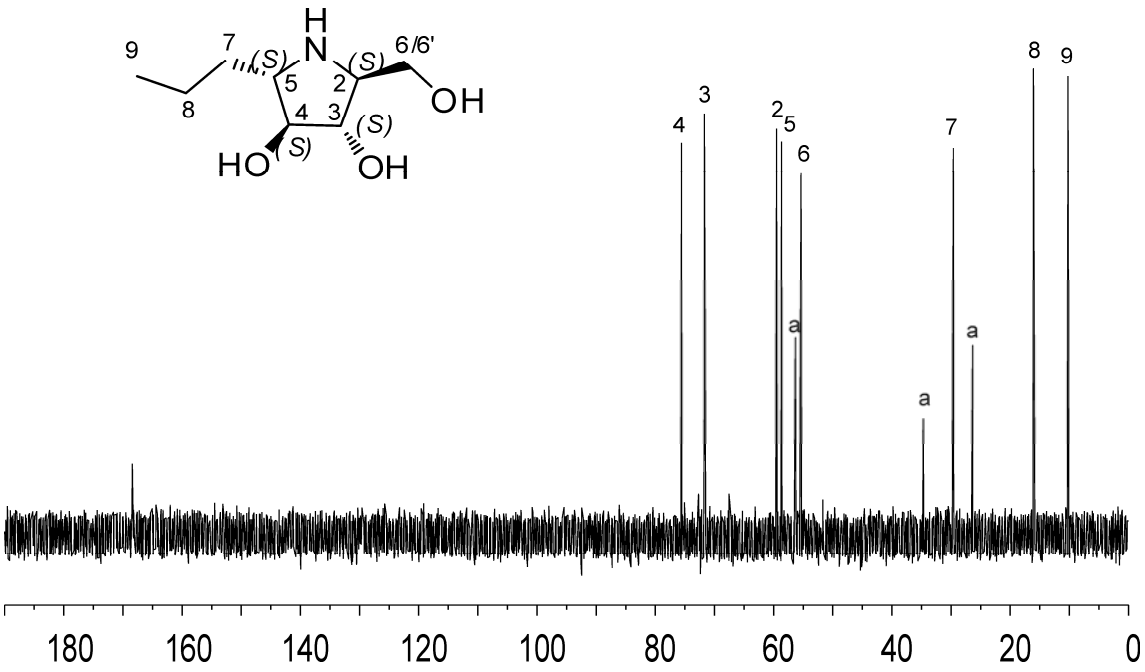
H
N
9
7
(S)
5
2
6/6'
(S)
OH
8
4
3
(S)
HO
(S)
OH
4
3
2
5
6
a
a
7
a
8
9
180
160
140
120
100
80
60
40
20
0

Figure S11. Observed ^{1}H and ^{13}C NMR spectra of the iminocyclitol resulted from the reductive amination of the aldol adduct from the aldol addition of DHA to (*R*)-**1d** catalyzed by RhuA in the presence of borate.

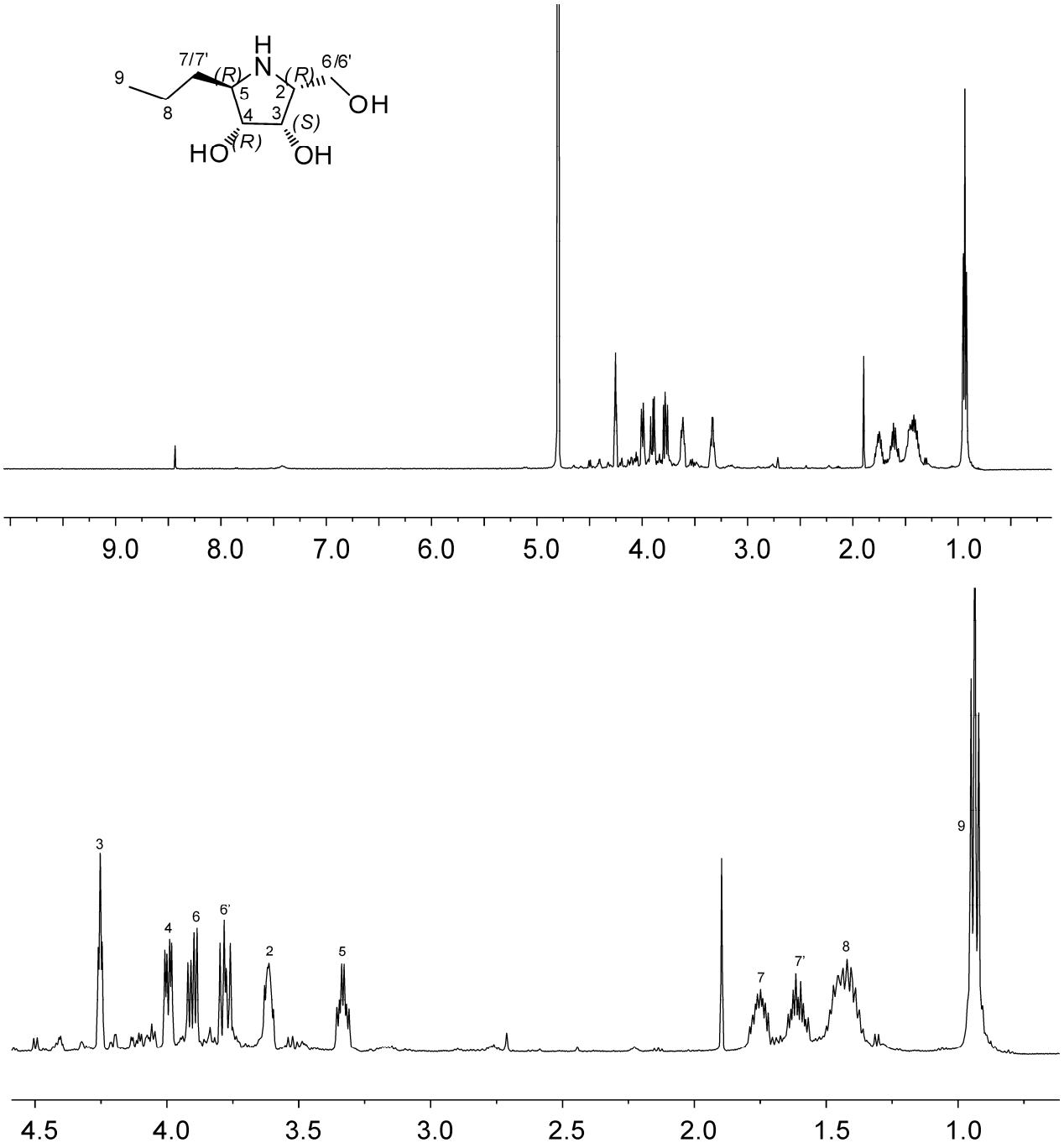

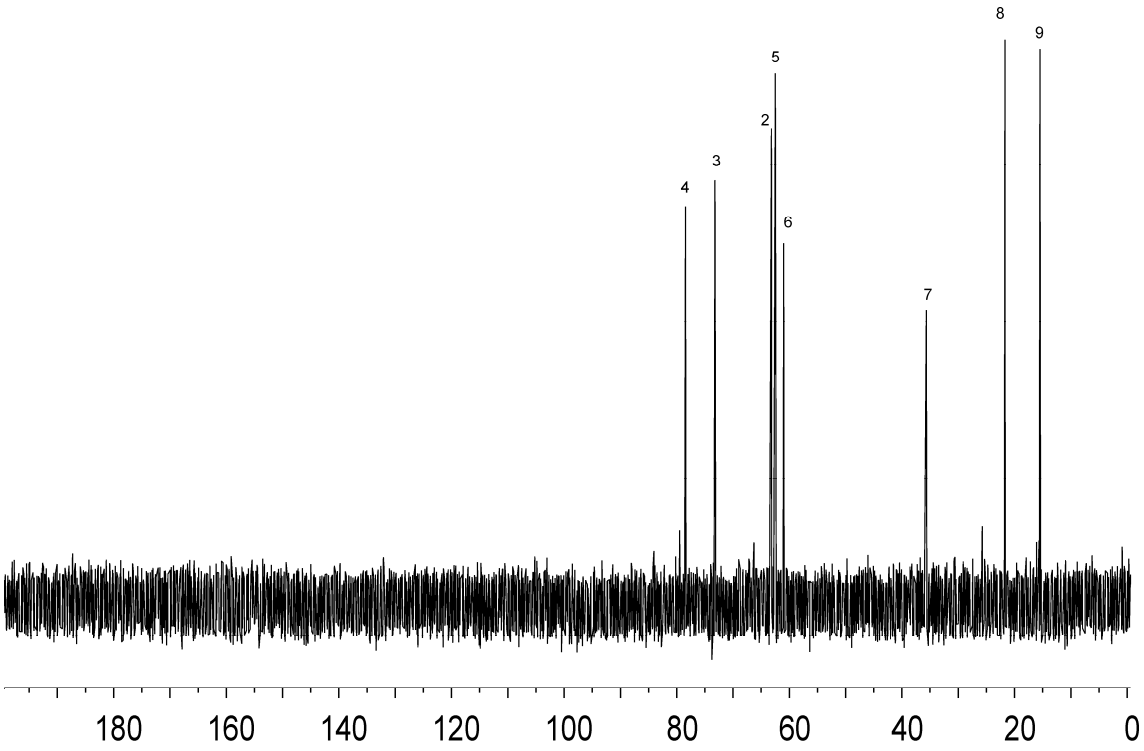

Figure S12. Observed ^{1}H and ^{13}C NMR spectra of the iminocyclitol resulted from the reductive amination of the aldol adduct from the aldol addition of DHA to (*S*)-**1e** catalyzed by RhuA in the presence of borate.

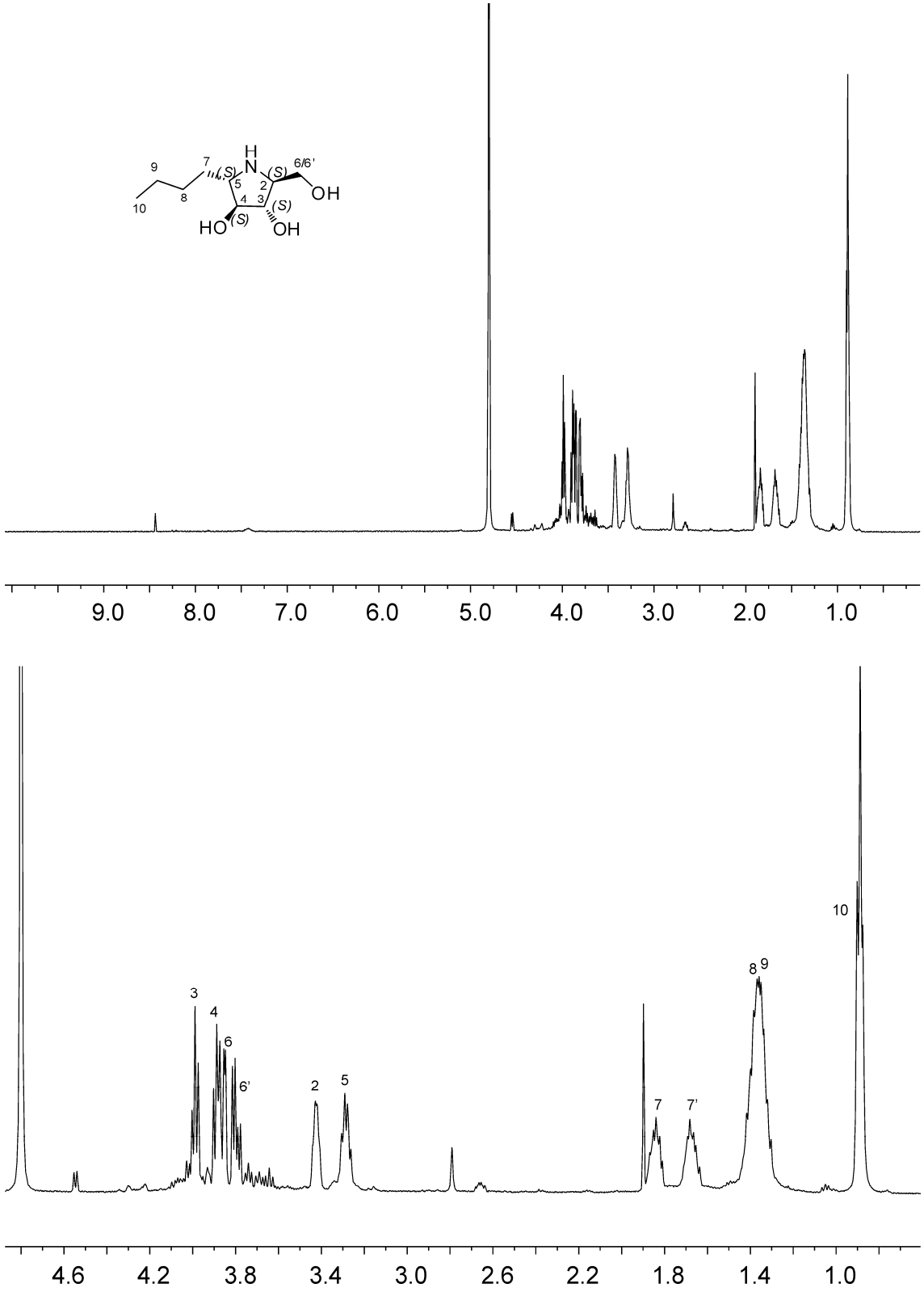

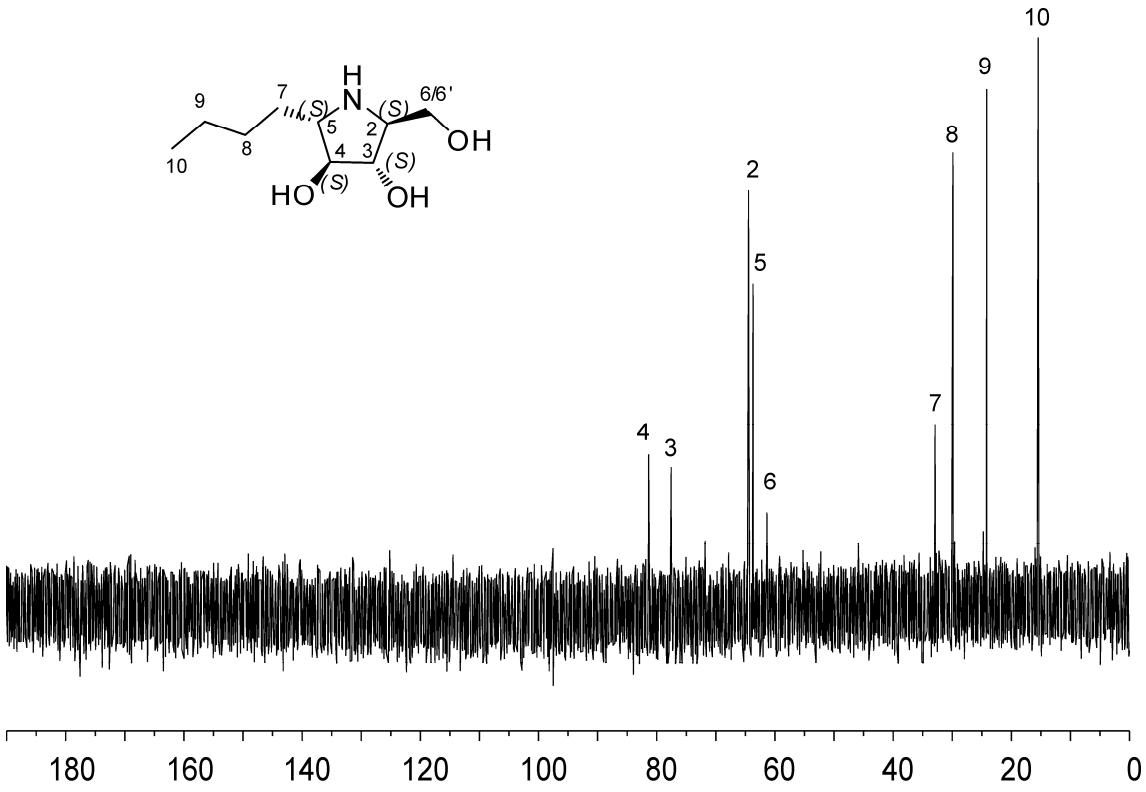
H
N
9
7
(S)
5
2
(S)
6/6'
OH
10
8
4
3
(S)
HO
(S)
OH
10
9
8
2
5
7
4
3
6
180
160
140
120
100
80
60
40
20
0

Figure S13. Observed ^{1}H and ^{13}C NMR spectra of the iminocyclitol resulted from the reductive amination of the aldol adduct from the aldol addition of DHA to (*R*)-**1e** catalyzed by RhuA in the presence of borate.

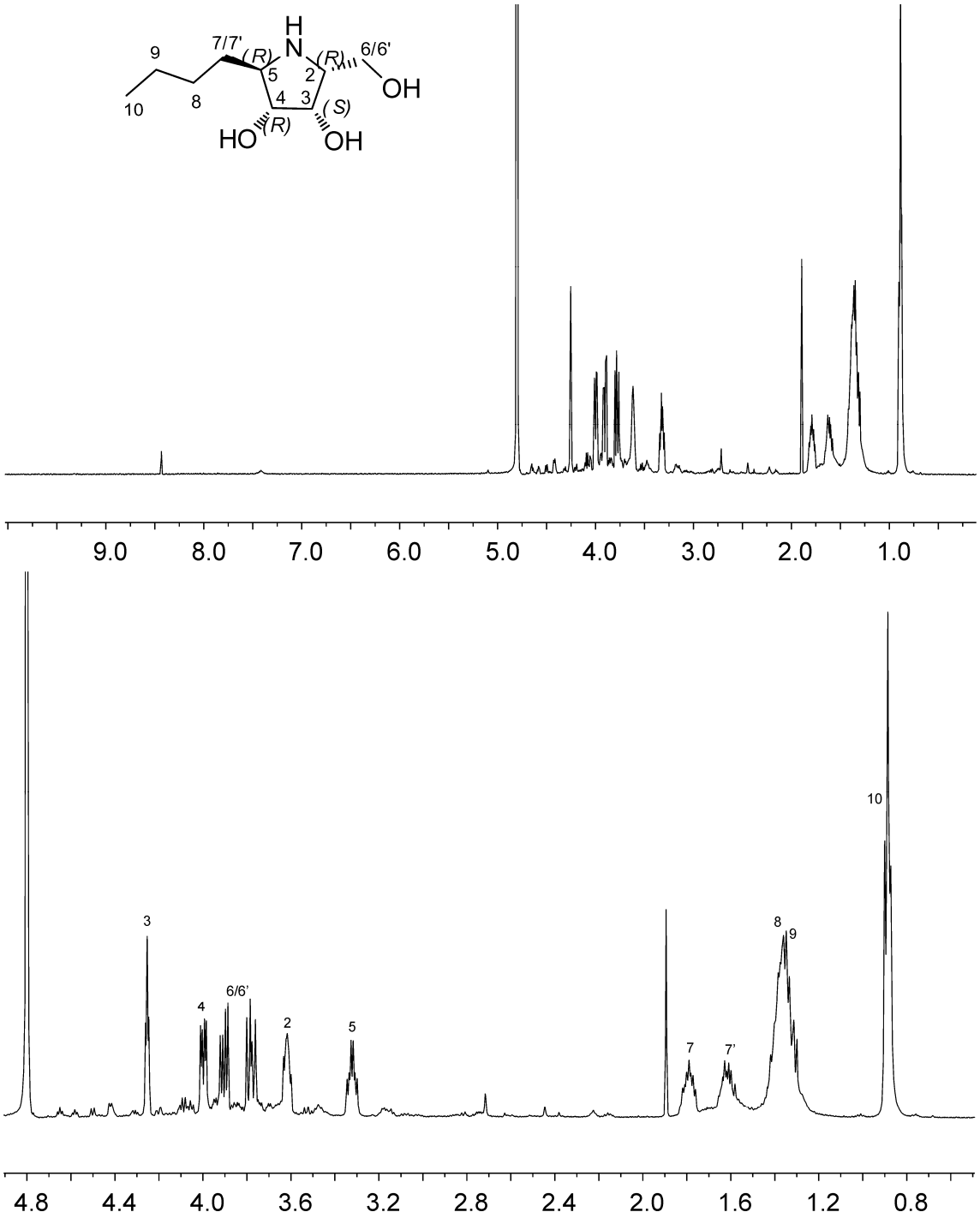

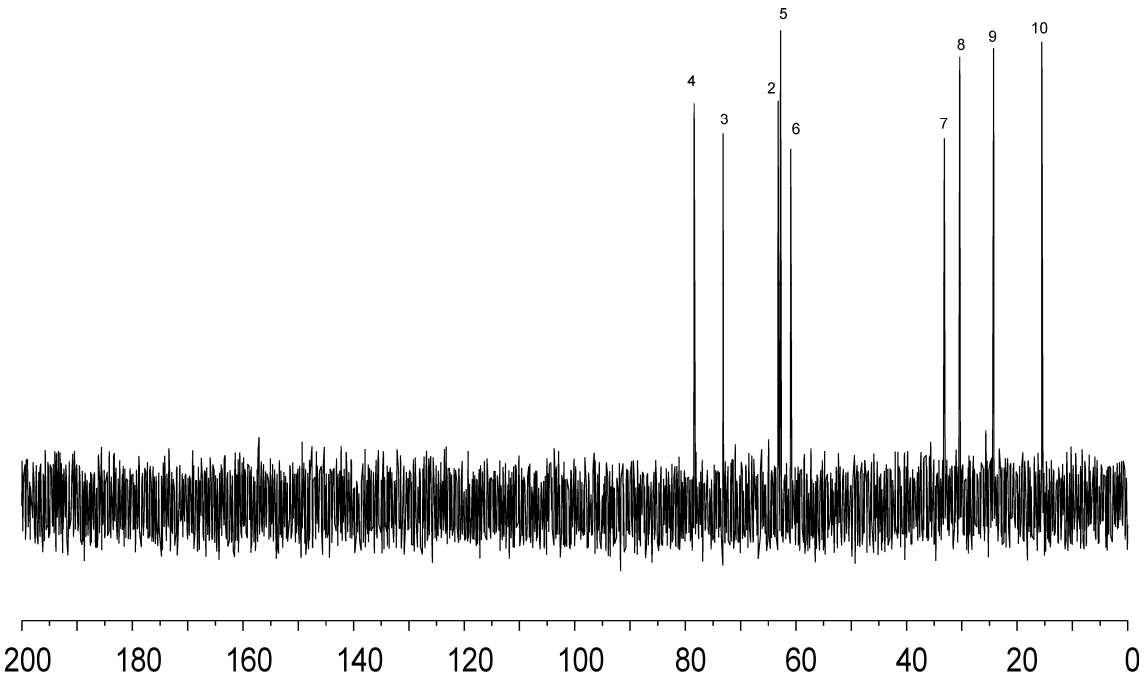

Figure S14. Observed ^{1}H and ^{13}C NMR spectra of the iminocyclitol resulted from the reductive amination of the aldol adduct from the aldol addition of DHA to (*R*)-**1f** catalyzed by RhuA in the presence of borate.

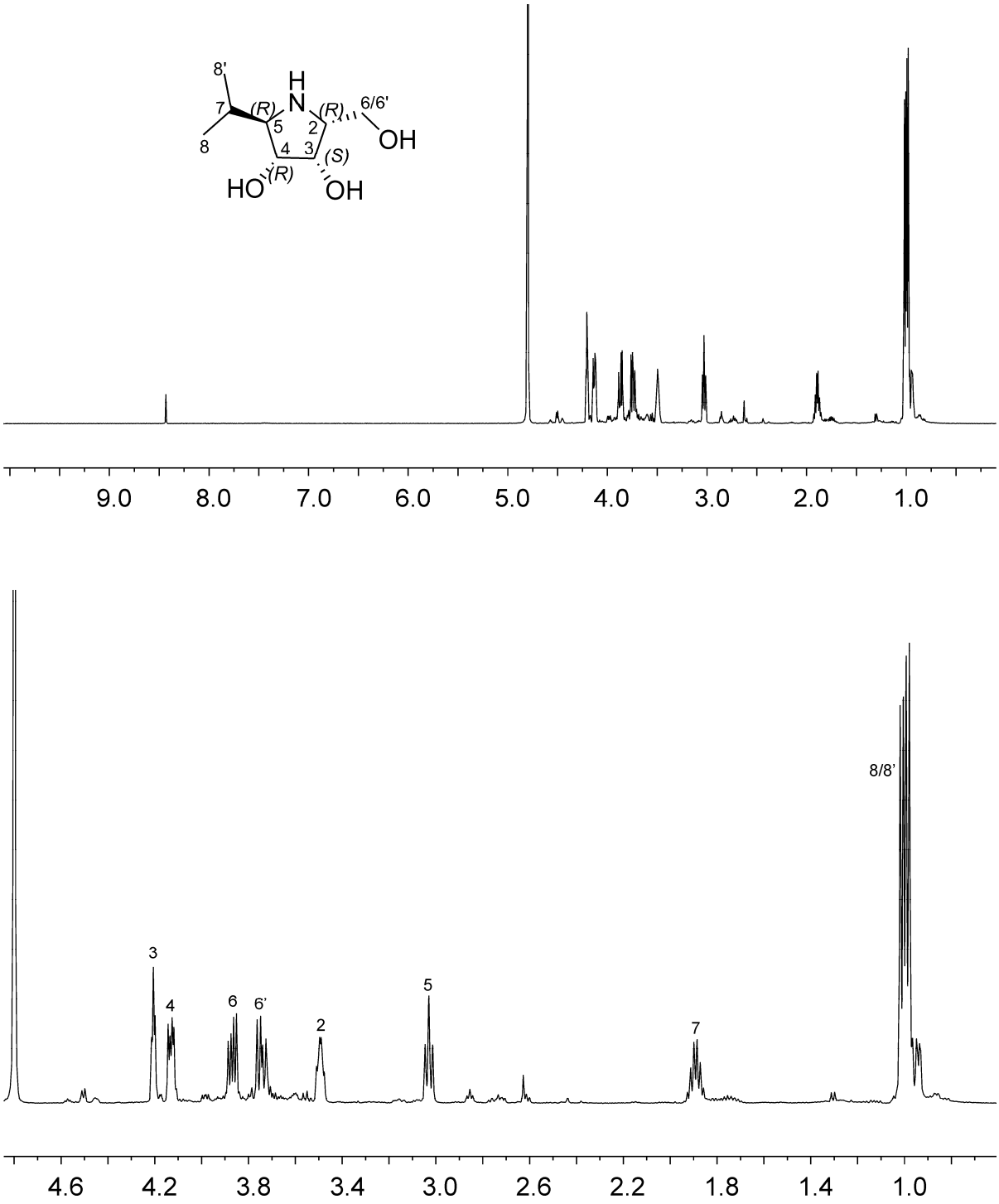

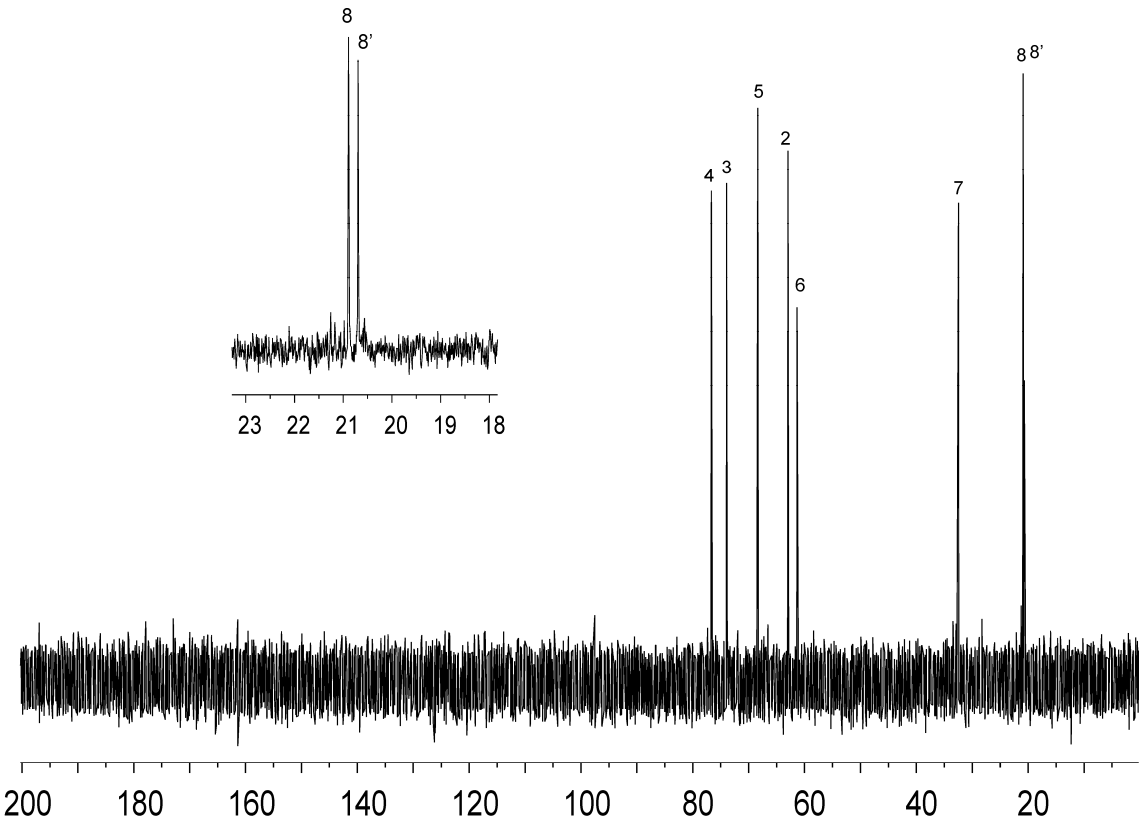

Figure S15. Observed ^{1}H and ^{13}C NMR spectra of the iminocyclitol resulted from the reductive amination of the aldol adduct from the aldol addition of DHA to (*R*)-**1h** catalyzed by RhuA in the presence of borate.

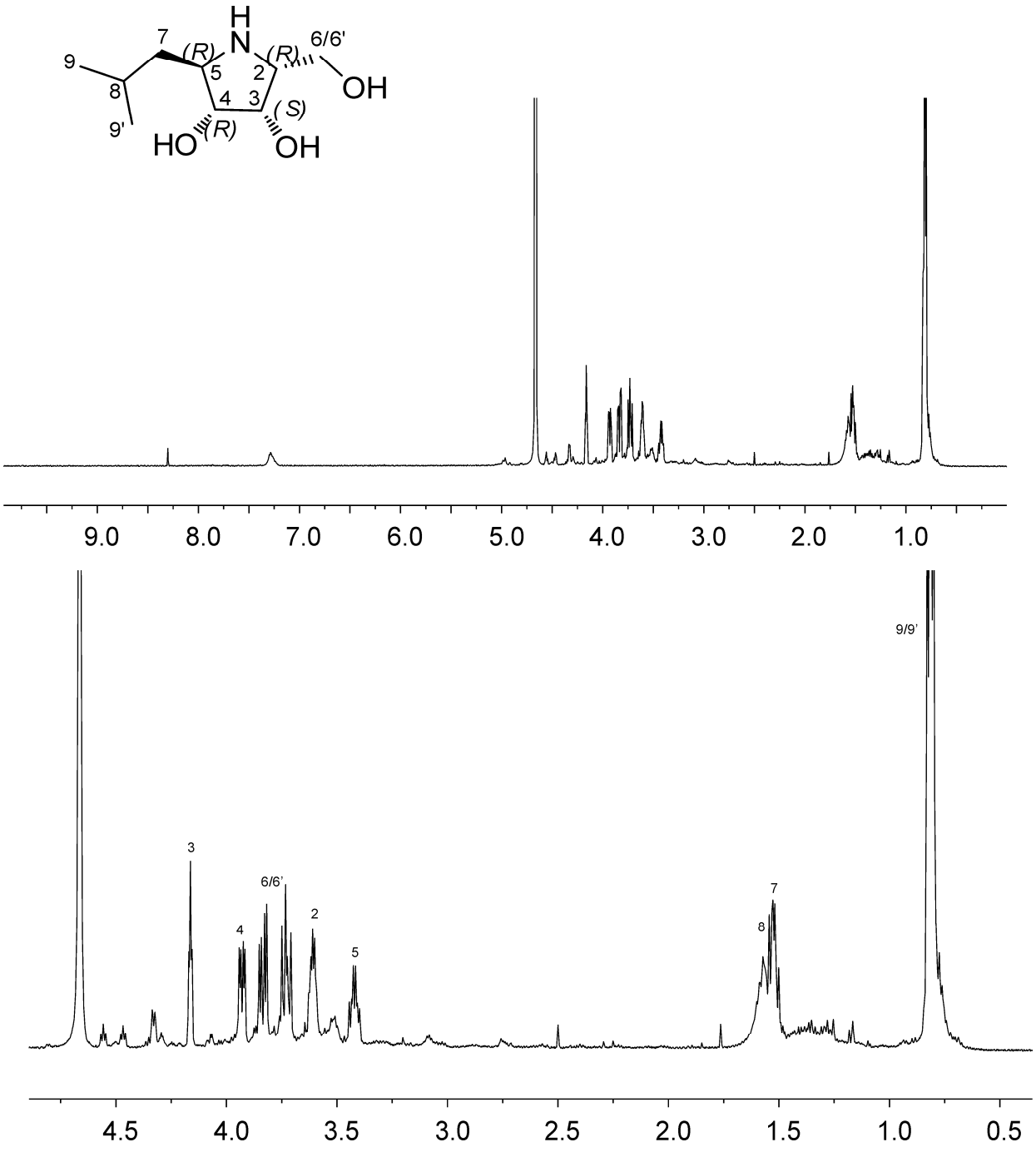

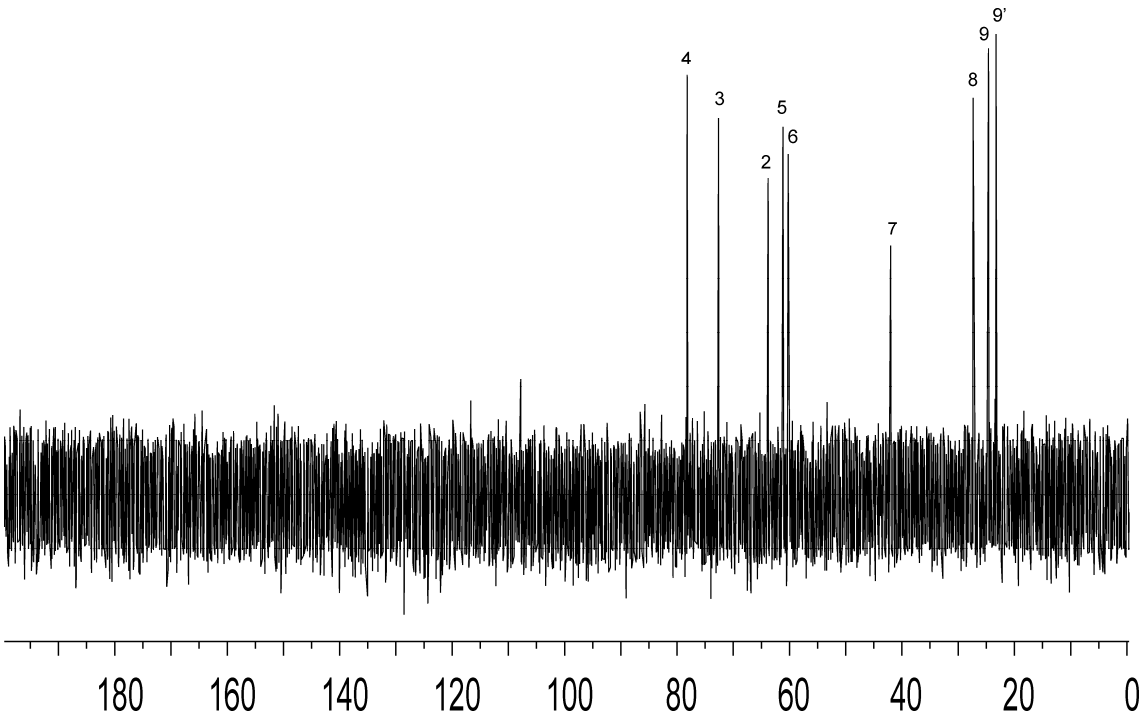

Figure S16. Observed ^{1}H and ^{13}C NMR spectra of the iminocyclitol resulted from the reductive amination of the aldol adduct from the aldol addition of DHA to **1i** catalyzed by RhuA in the presence of borate.

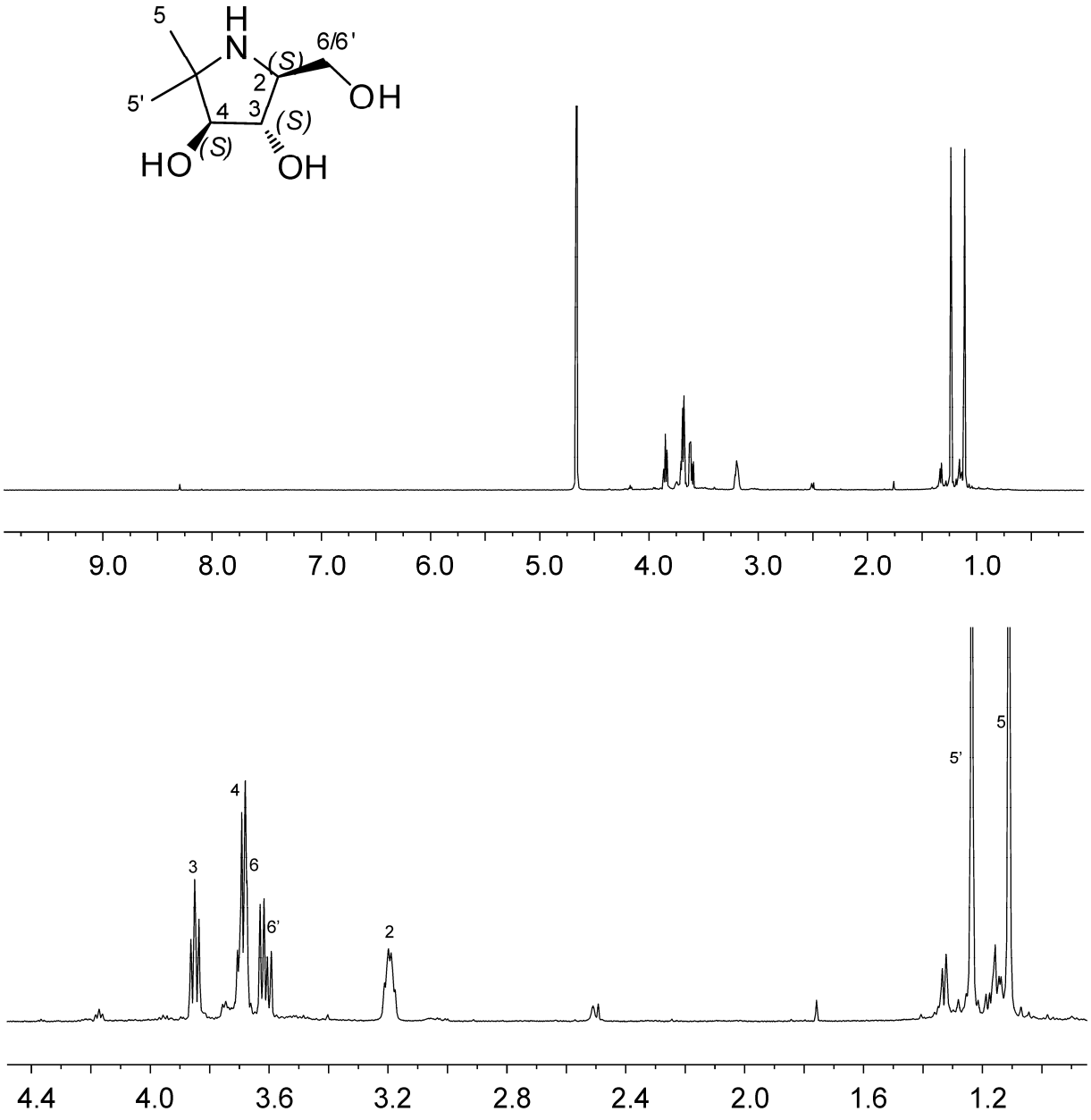

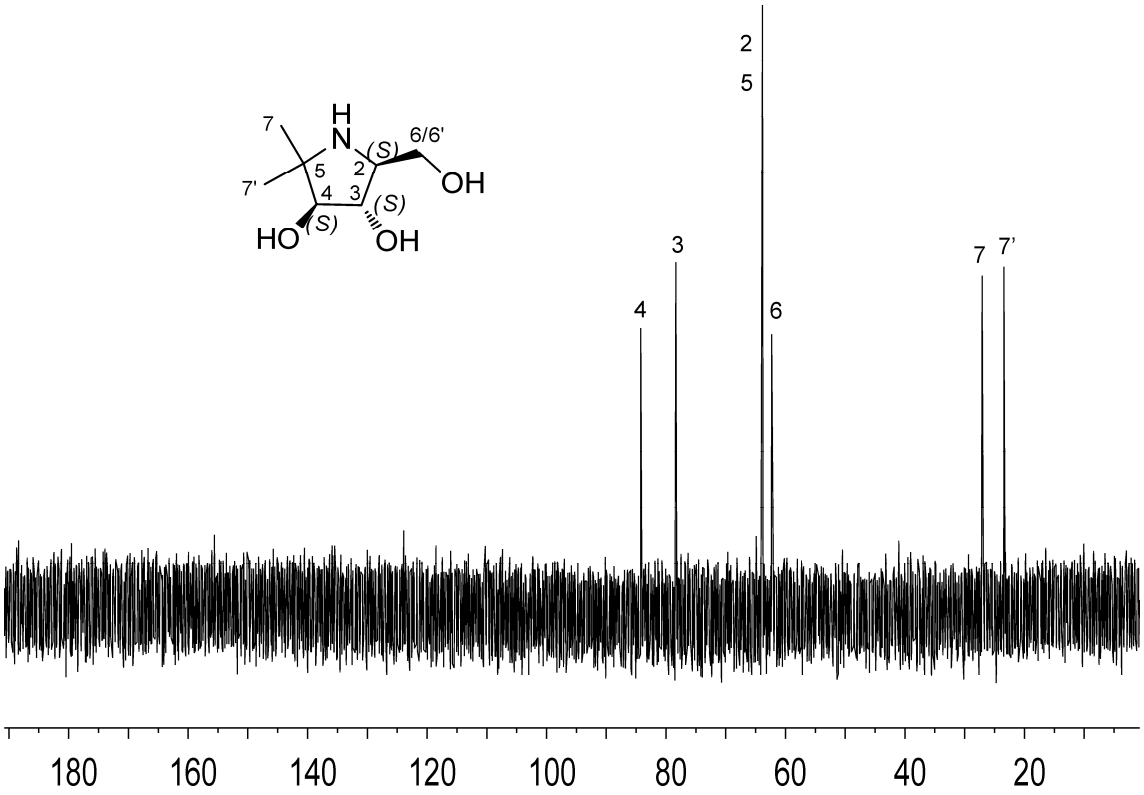
H
N
7
7'
5
4
3
2
(S)
(S)
(S)
6/6'
OH
HO
OH
2
5
4
3
6
7
7'
180
160
140
120
100
80
60
40
20

Figure S17. ^{1}HNMR spectra of the aldol adduct resulted from the aldol addition reaction of DHA to **1j** in the presence of borate.

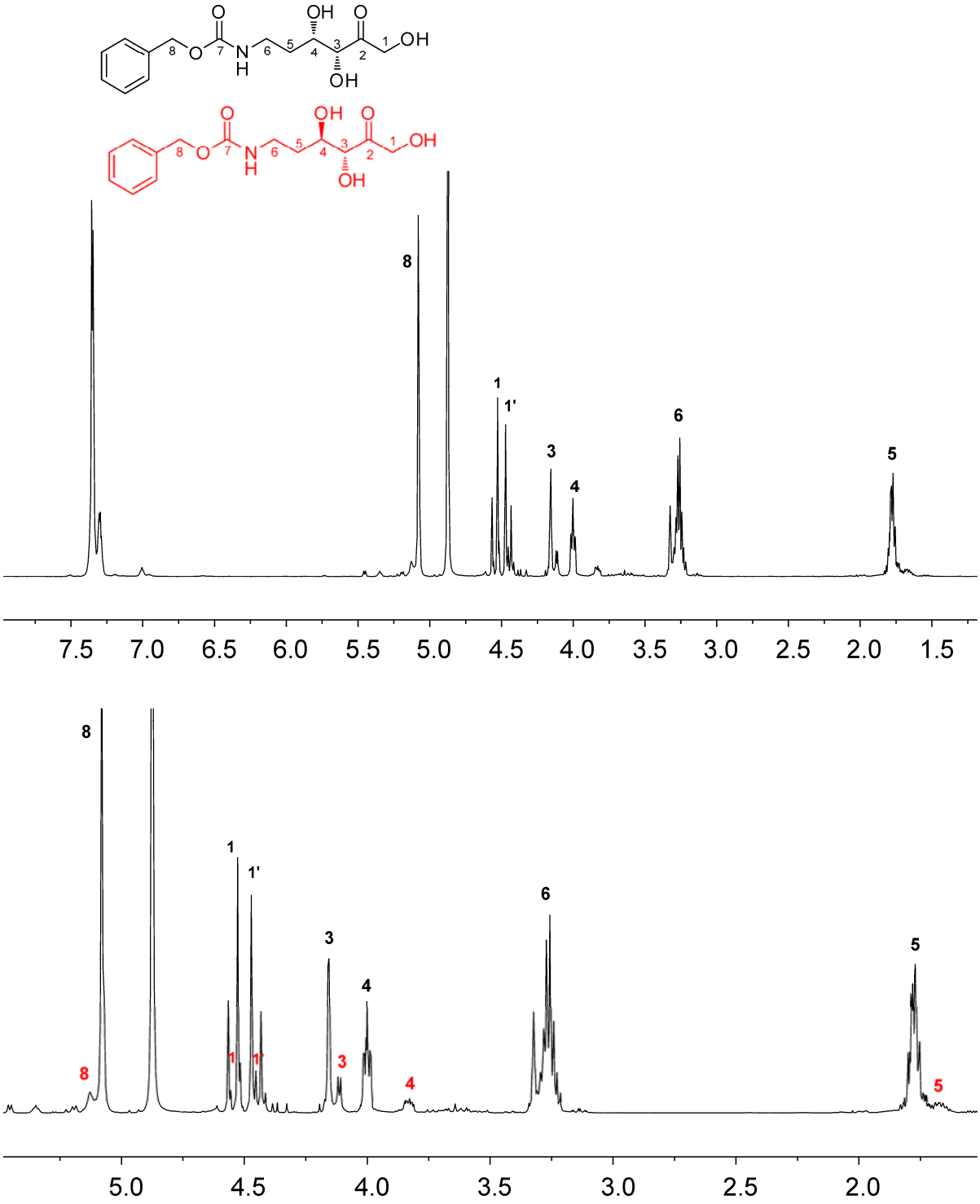

Molecular modelling

In order to determine which of the potential borate complexes derived from the cyclic hemiaminal (3*R*,4*S*,5*S*)-**2b** could be preferentially formed, we carried out calculations at the B3LYP / 6-31G** level to determine the relative free energies in solution of several BL and BL_2 complexes,[6] namely those from α,β- and α,γ-bidentate BL complexes and combinations of α,β/α,β-, α,β/α,γ- and α,γ /α,γ- BL_2 complexes (i.e., combinations are restricted to those derived from low energy α,β- or α,γ-BL complexes). Chart S1 and Table S4 show the structures and results obtained for the different BL complexes considered. α,β-Bidentate complexes **I** and **VII** resulted as the most stable BL borate esters, while borates **II**, **III** and **IV**, derived from *trans* α,β-diols, are the less energetically favoured, as expected.[7] Similarly, the *trans* α,γ-bidentate BL complex **V** is less stable than its *cis* homolog **VI**. Chart S2 and Table S5 show the structures and results obtained for the different BL_2 complexes considered. Among them, complex **I-Ia** appears to be the most stable in solution.

All calculations were carried out with the package Schrödinger Suite 2009 (Schrödinger, LLC, New York) through its graphical interphase Maestro (Maestro, version 9.0, Schrödinger, LLC, New York, NY, 2009). Conformational searches were carried out using the mixed MCMM/LMCS method[8] implemented in the program MacroModel (MacroModel, version 9.7, Schrödinger, LLC, New York, NY, 2009), with the default force field OPLS 2005, a modified version of the OPLS-AA force field.[9] The lowest energy minima detected in each case were subjected to further minimization at the DFT (B3LYP/6-31G**) level with the program Jaguar (Jaguar, version 7.6, Schrödinger, LLC, New York, NY, 2009). Vibrational frequencies were calculated to characterize the nature of the determined stationary points as minima (no imaginary frequency) and to calculate the zero-point energies (ZPE) as well as the

thermal and entropic corrections. Single point energy calculations under implicit water solvation were carried out by using the standard Poisson-Boltzmann solver[10, 11] included in Jaguar to determine the solvation energy, which was used to calculate the Gibbs free energies in solution.

Chart S1. Structures of potential BL borate complexes that can be formed from the cyclic hemiaminal derived from adduct (3*R*,4*S*,5*S*)-**2b**.

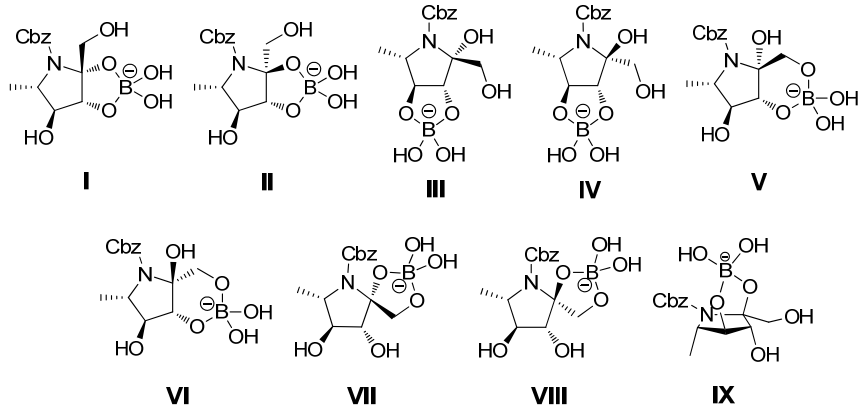

Table S4. Gas phase energy (E^{gp}, hartrees), zero point energy (ZPE, kcal mol^{-1}), enthalpic (ΔH, kcal mol^{-1}) and entropic (ΔS, cal mol^{-1}) corrections at 298.15 K, solvation energy (E^{sol}, kcal mol^{-1}) and relative Gibbs free energies (ΔG^{wat}, kcal mol^{-1}) in water solution of the most stable conformers determined for structures of BL borate complexes **I-IX**.

	E^{gp}	ZPE	ΔH	ΔS	E^{sol}	ΔG^{wat}
I	-1226.572523	215.46	14.13	153.96	-73.38	0.00
II	-1226.545899	214.80	14.40	154.14	-64.96	24.68
III	-1226.546084	215.09	14.24	153.69	-71.32	18.47
IV	-1226.540088	214.52	14.59	157.01	-73.22	19.13
V	-1226.568886	215.59	13.99	153.26	-70.25	5.62
VI	-1226.572470	215.45	13.45	146.11	-70.59	4.47
VII	-1226.571938	215.57	14.02	152.61	-73.73	0.41
VIII	-1226.576733	215.43	13.54	147.23	-70.13	2.00
IX	-1226.566382	215.63	14.08	151.88	-69.77	8.21

Chart S2. Structures of potential BL_2 borate complexes that can be formed from the cyclic hemiaminal derived from adduct (3*R*,4*S*,5*S*)-**2b**.

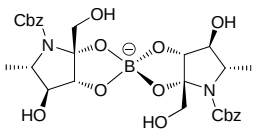
I-Ia

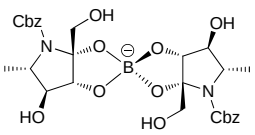
I-Ib

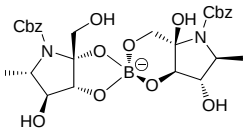
I-Va

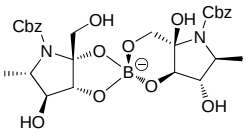
I-Vb

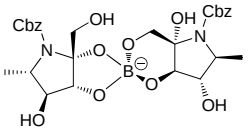
I-VIa

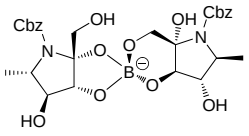
I-VIb

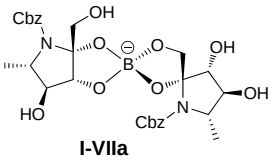
I-VIIa

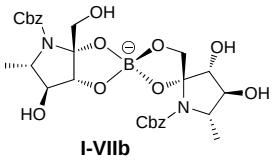
I-VIIb

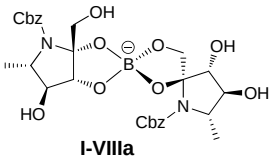
I-VIIIa

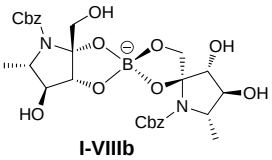
I-VIIIb

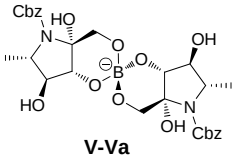
V-Va

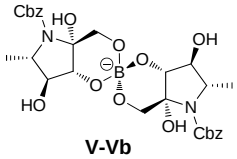
V-Vb

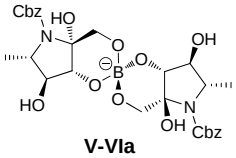
V-VIa

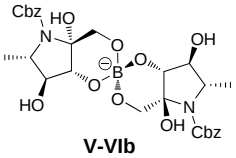
V-VIb

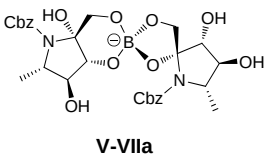
V-VIIa

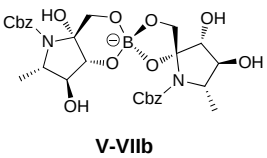
V-VIIb

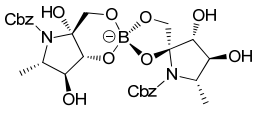
V-VIIIa

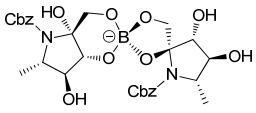
V-VIIIb

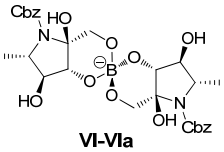
VI-VIa

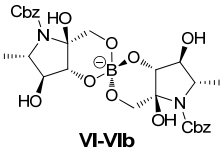
VI-VIb

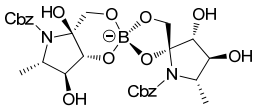
VI-VIIa

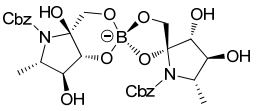
VI-VIIb

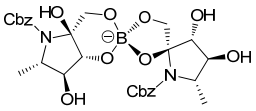
VI-VIIIa

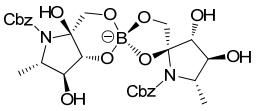
VI-VIIIb

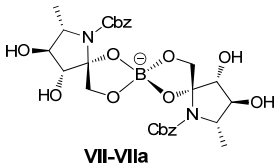
VII-VIIa

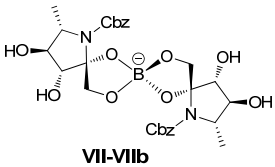
VII-VIIb

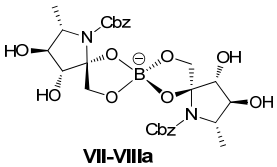
VII-VIIIa

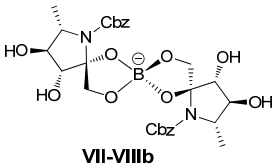
VII-VIIIb

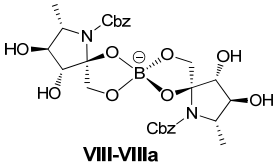
VIII-VIIIa

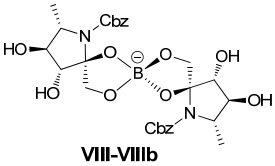
VIII-VIIIb

Table S5. Gas phase energy (E^{gp}, hartrees), zero point energy (ZPE, kcal mol^{-1}), enthalpic (ΔH, kcal mol^{-1}) and entropic (ΔS, cal mol^{-1}) corrections at 298.15 K, solvation energy (E^{sol}, kcal mol^{-1}) and relative Gibbs free energies (ΔG^{wat}, kcal mol^{-1}) in water solution of the most stable conformers determined for structures of borate BL_2 complexes.

	E^{gp}	ZPE	ΔH	ΔS	E^{sol}	ΔG^{wat}
I-Ia	-2124.801073	390.17	23.99	227.83	-67.23	0.00
I-Ib	-212.4.798924	390.52	23.63	222.07	-57.42	12.86
I-Va	-2124.791220	390.55	23.08	218.72	-65.46	10.14
I-Vb	-2124.787704	390.91	22.96	217.34	-68.97	9.49
I-VIa	-2124.795032	390.94	23.36	221.79	-62.92	10.05
I-VIb	-2124.797904	390.35	23.71	224.73	-62.98	7.06
I-VIIa	-2124.796528	390.84	23.47	220.25	-66.24	6.25
I-VIIb	-2124.803140	390.69	24.15	227.81	-59.30	7.32
I-VIIIa	-2124.802926	390.93	24.09	226.79	-62.20	5.04
I-VIIIb	-2124.797154	390.45	23.72	223.37	-60.89	10.14
V-Va	-2124.779917	390.96	22.40	211.21	-67.19	17.47
V-Vb	-2124.780630	391.15	23.43	222.68	-65.72	16.30
V-VIa	-2124.779645	390.96	22.87	215.72	-67.11	16.85
V-VIb	-2124.785857	390.99	23.41	223.28	-61.86	16.52
V-VIIa	-2124.792046	390.62	23.51	221.50	-63.69	11.05
V-VIIb	-2124.790115	390.72	23.47	221.40	-62.62	13.43
V-VIIIa	-2124.793637	390.71	23.51	221.10	-57.86	16.10
V-VIIIb	-2124.791728	391.00	23.95	225.92	-61.32	13.13
VI-VIa	-2124.796620	390.52	23.50	222.63	-60.53	10.91
VI-VIb	-2124.788439	390.74	23.42	221.41	-63.09	13.99
VI-VIIa	-2124.792333	390.40	23.66	223.92	-61.71	12.08
VI-VIIb	-2124.791046	390.58	23.51	222.38	-66.17	8.91
VI-VIIIa	-2124.799382	390.49	23.49	220.05	-58.32	12.11
VI-VIIIb	-2124.795018	390.89	23.32	220.09	-60.79	12.61
VII-VIIa	-2124.798709	390.18	23.70	221.09	-63.73	6.70

VII-VIIb	-2124.774617	390.35	23.18	217.29	-63.45	22.90
VII-VIIIa	-2124.800341	390.73	23.42	219.64	-60.82	9.31
VII-VIIIb	-2124.799998	390.41	24.15	228.74	-59.13	8.91
VIII-VIIIa	-2124.801378	390.81	24.64	235.08	-59.44	6.72
VIII-VIIIb	-2124.802492	390.34	23.68	222.02	-54.74	13.19

References

1. L. Espelt, T. Parella, J. Bujons, C. Solans, J. Joglar, A. Delgado and P. Clapés, *Chem. Eur. J.*, 2003, **9**, 4887-4899.
2. J. Calveras, M. Egido-Gabás, L. Gómez, J. Casas, T. Parella, J. Joglar, J. Bujons and P. Clapés, *Chem. Eur. J.*, 2009, **15**, 7310-7328.
3. J. Calveras, J. Casas, T. Parella, J. Joglar and P. Clapés, *Adv. Synth. Catal.*, 2007, **349**, 1661-1666.
4. X. Garrabou, L. Gomez, J. Joglar, S. Gil, T. Parella, J. Bujons and P. Clapés, *Chem. Eur. J.*, 2010, **16**, 10691-10706.
5. M. M. Bradford, *Anal. Biochem.*, 1976, **72**, 248-254.
6. J. E. Sponer, B. G. Sumpter, J. Leszczynski, J. Sponer and M. Fuentes-Cabrera, *Chem. Eur. J.*, 2008, **14**, 9990-9998.
7. R. van den Berg, J. A. Peters and H. van Bekkum, *Carbohydr. Res.*, 1994, **253**, 1-12.
8. I. Kolossvary and W. C. Guida, *J. Comput. Chem.*, 1999, **20**, 1671-1684.
9. W. L. Jorgensen, D. S. Maxwell and J. Tirado-Rives, *J. Am. Chem. Soc.*, 1996, **118**, 11225-11236.
10. D. J. Tannor, B. Marten, R. Murphy, R. A. Friesner, D. Sitkoff, A. Nicholls, B. Honig, M. Ringnalda and W. A. Goddard, III, *J. Am. Chem. Soc.*, 1994, **116**, 11875-11882.
11. B. Marten, K. Kim, C. Cortis, R. A. Friesner, R. B. Murphy, M. N. Ringnalda, D. Sitkoff and B. Honig, *J. Phys. Chem.*, 1996, **100**, 11775-11788.